



UNIVERSIDADE D  
COIMBRA

Ana Maria Reis Costa

**THE IMPACT OF DIFFERENT LIPOGENIC DIETS ON  
DIRECT AND INDIRECT PATHWAY CONTRIBUTIONS  
TO HEPATIC GLYCOGEN SYNTHESIS**

**Dissertação no âmbito do Mestrado em Biologia Celular e Molecular  
orientada pelo Professor Doutor John Griffith Jones e pelo Professor Doutor  
Rui de Albuquerque Carvalho e apresentada ao Departamento de Ciências da  
Vida da Faculdade de Ciências e Tecnologia da Universidade de Coimbra.**

Outubro de 2020



Faculdade de Ciências e Tecnologia da Universidade de Coimbra

# The impact of different lipogenic diets on direct and indirect pathway contributions to hepatic glycogen synthesis

Ana Maria Reis Costa

Dissertação no âmbito do Mestrado em Biologia Celular e Molecular orientada pelo Professor Doutor John Griffith Jones e pelo Professor Doutor Rui de Albuquerque Carvalho e apresentada ao Departamento de Ciências da Vida da Faculdade de Ciências e Tecnologia da Universidade de Coimbra.

Outubro de 2020



UNIVERSIDADE D  
COIMBRA



## Acknowledgements

---

This has been a really tough year for too many reasons and I truly feel I need to appreciate everyone that helped me get through it, especially those who have impacted this thesis or my academic life to some extent.

To the Metabolic Control Group for the help, support, and friendship. It has been an honor to meet and work with each and every one of you, but especially with Doctor Ludgero Tavares and Doctor John Jones. To Doctor Ludgero, my mentor in the lab, I want to thank you not only for all the hours you have spent teaching me NMR (or at least trying to) but also for all the advice and for always pushing me to go further and excel. Thank you for not giving up on me and for being always ready to help, even with a pandemic going on. To Professor John Jones, thank you so much for believing in me when no one else did, for being always available to help, and for all your expertise and patience during the last few weeks. I couldn't have asked for a better supervisor.

To Professor Rui de Carvalho, thank you for introducing me to metabolism in your classes. It inspired me so much that I ended up choosing this field and working with you. I also need to appreciate you for reminding me constantly that your lab was an open door for anything I needed.

Now I am switching to Portuguese because I don't think it makes sense to address most of these people in a language that is not their own.

A Coimbra, quero agradecer por me ter escolhido em 2014, quando esta não tinha sido a minha primeira escolha. Aqui, conheci pessoas incríveis e experienciei momentos inesquecíveis. À Magda e à Serdoura, que estiveram presentes desde o início e viveram grande parte dos momentos mais marcantes da minha vida nos últimos 6 anos. Sinto mesmo que vocês são parte da minha família. Um obrigada muito especial à Magda, por tomar conta de toda a gente e garantir que ninguém “atira a toalha ao chão”. À Maria, por todo o apoio e companheirismo. Acredito que partilhar casa comigo este ano não tenha sido muito fácil, especialmente na era COVID. Obrigada também por toda a paciência a explicar-me Física e por todas as vezes que ouviste os meus desabafos. Ao Pedro, por fazer o longe perto e nunca desistir de mim, apesar de ser provavelmente um dos meus maiores críticos. Acho que és a pessoa que melhor conhece as

dificuldades que tive ao escrever este documento e que, conseqüentemente, mais me apoiou e, por isso, estarei sempre grata.

Ao meu Algarve, por me receber sempre de braços abertos. Aos meus amigos, Alexandre e Joana, por demonstrarem que as amizades sobrevivem ao tempo e que a distância é só um número. À Carla, por ser a amiga de todas as horas e me provar inúmeras vezes que existem laços tão fortes como os familiares, mesmo não havendo sangue à mistura.

À minha família, por serem os meus maiores fãs e por nunca desistirem de mim. Obrigada por toda a ajuda emocional e financeira, mesmo não sabendo exatamente aquilo que eu faço ou ambiciono fazer. Mãe, pai, mana e avó, obrigada por aceitarem e compreenderem todas as minhas ausências. Espero sempre orgulhar-vos e que o vosso esforço não seja em vão.

Financial support from the Portuguese Foundation for Science and Technology (research grant FCT-FEDER-02/SAICT/2017/028147) and from the Portuguese Society for Diabetology Fundamental and Translational Investigation Study Group (SPD-GIFT). Structural funding for the Center for Neurosciences and Cell Biology and the UC-NMR facility is supported in part by FEDER – European Regional Development Fund through the COMPETE Program, Centro 2020 Regional Operational Program, and the Portuguese Foundation for Science and Technology through grants UIDB/04539/2020; POCI-01-0145-FEDER-007440; REEQ/481/QUI/2006, RECI/QEQ-QFI/0168/2012, CENTRO-07-CT62-FEDER-002012, and Rede Nacional de Ressonância Magnética Nuclear.

To my family, but especially to José Miguel,

I don't have the solution, but one day I may have some answers.

# Index

---

Acknowledgements.....	3
Index.....	6
List of Figures .....	8
Abbreviations .....	10
Abstract .....	14
Resumo.....	15
Introduction .....	17
Non-Alcoholic Fatty Liver Disease .....	17
Diagnosis and prognosis.....	18
Treatment.....	20
Endocrine and nutritional players in NAFLD .....	20
The Insulin/Glucagon ratio.....	21
Insulin .....	22
Glucagon.....	23
Different roles of Irs1 and Irs2 in the insulin signalling cascade .....	24
Insulin resistance in NAFLD .....	26
Lipids as molecular drivers of insulin resistance .....	27
Hepatic insulin resistance modulates $\beta$ -cell hyperplasia .....	29
Paradoxes of hepatic insulin resistance, fatty acid oxidation and lipogenesis in NAFLD .....	30
The effect of diet composition in the obesity epidemic and the consequences for NAFLD – The threats of sugar and fructose .....	30
Glycogen Metabolism .....	35
Importance .....	35
Glycogenesis and the “Glucose Paradox” .....	35
Glycogenolysis .....	38
Glycogen synthase and Glycogen phosphorylase interdependency .....	40
Glycogen cycling.....	40
Glycogen Metabolism and Endocrine Control dysregulation .....	41
Glycogen storage disease type I (GSD-I) .....	41
Maturity onset diabetes mellitus of the young type 2 (MODY2).....	41
Insulin-dependent diabetes mellitus (IDDM).....	42
NAFLD .....	42



Possible role of hepatic glycogen in the neuroendocrine regulation of food intake – The liver-brain axis .....	43
Methods for measuring total glycogen synthesis and hydrolysis rates.....	44
Animal models to study NAFLD.....	45
Genetic models of NAFLD .....	46
Dietary models of NAFLD .....	47
Objectives.....	50
Materials and Methods.....	51
Reagents.....	51
Experimental models and management.....	52
Glycogen extraction, derivatization and purification to monoacetone glucose (MAG) .....	54
1. Glycogen extraction .....	54
2. Glycogen digestion to glucose.....	54
3. Glucose derivatization to MAG .....	55
4. MAG purification .....	55
Glycogen quantification .....	55
NMR experiments .....	56
Deuterium and Carbon-13 spectra acquisition parameters .....	56
Metabolic Flux evaluation.....	56
1. Glycogen deuterium enrichment .....	56
2. Glycogen <sup>13</sup> C-enrichment derived from [U- <sup>13</sup> C <sub>6</sub> ]fructose.....	59
Statistical analysis .....	61
Results.....	63
1. Hepatic Glycogen quantification.....	63
2. Sources of hepatic glycogen synthesis.....	63
3. Carbon-13 Isotopomers NMR analysis.....	67
Discussion.....	69
Conclusion.....	73
References.....	75

## List of Figures

---

**Figure 1** World distribution of NAFLD patients adapted from Younossi, Z. et al. (2019). The highest incidence is registered in the Middle East and South America, followed by Asia, North America and Europe. The lowest incidence is verified in Africa.<sup>3</sup> ..... 17

**Figure 2** Schematic illustrating disease progression. NAFL is characterized by triglyceride accumulation within lipid droplets and NASH by fibrosis and inflammatory infiltration. NASH patients can progress to cirrhosis and ultimately to HCC..... 18

**Figure 3** Schematic representation of Glycolysis and Fructolysis, including the intervenient enzymes. The enzymes in blue belong to Glycolysis, while those in purple belong to Fructolysis. .... 32

**Figure 4** Schematic representing the direct and indirect pathways of glycogen synthesis. .... 38

**Figure 5** Schematic representing the pathway of glycogen oxidation with the intervenient enzymes described. .... 39

**Figure 6** Representative <sup>2</sup>H-NMR spectrum of MAG obtained from the hepatic glycogen of a C57/BL6 mouse included in this study. The peaks corresponding to the possible deuterium enriched positions in the molecule which were used for the analysis are H5 and H6S. .... 57

**Figure 7** Representative <sup>2</sup>H-NMR spectrum of plasma obtained from a C57/BL6 mouse included in this study. The peak on the right corresponds to the natural-abundance <sup>2</sup>H from the methyl hydrogen of acetone, which serves as an internal enrichment standard, and the one on the left is from the water hydrogens. The relationship between the acetone and water signals is established beforehand by performing a calibration curve with known <sup>2</sup>H-enriched water standards and is also adjusted for the plasma protein content (assumed to be 3% of total plasma weight). .... 58

**Figure 8** Carbon 5 multiplet from a representative <sup>13</sup>C-NMR spectrum of MAG obtained from the hepatic glycogen of a C57/BL6 mouse included in this study. The peaks corresponding to the quartet representing [4,5,6-<sup>13</sup>C<sub>3</sub>]glucose (C5Q456), the doublet from glucose enriched in both positions 4 and 5, [4,5-<sup>13</sup>C<sub>2</sub>]glucose (C5D45), the doublet from glucose enriched in both positions 5 and 6, 5,6-<sup>13</sup>C<sub>2</sub>]glucose (C5D56), and the singlet from the 1.11% natural-abundance <sup>13</sup>C (C5S) are labelled accordingly. .... 60

**Figure 9** Graph depicting the concentration of hepatic glycogen at the moment of the euthanization. Statistical analysis was performed using One-way ANOVA of multiple comparisons according to the Tukey's post-test. No statistically significant differences were identified. The + sign indicates the mean of each group and the triangle indicates

the maximum of the HS group, which is not an outlier. The amount of glycogen in SC mice was  $499 \pm 149 \mu\text{mol/g}$  of liver, in HF mice is  $371 \pm 113 \mu\text{mol/g}$  of liver, in HS mice is  $467 \pm 205 \mu\text{mol/g}$  of liver and in HFHS mice is  $487 \pm 142 \mu\text{mol/g}$  of liver..... 63

**Figure 10** Graph depicting the results of the evaluation the Indirect Pathway contribution to glycogen synthesis using  $^2\text{H}$ -enrichment NMR analysis of liver MAG. The statistical analysis performed in this case was One-way ANOVA of multiple comparisons with Tuckey's post-test, which indicates that the HF group is significantly different from the SC group ( $*p<0,05$ ), while the HS and HFHS mice are statistically different from the HF group ( $*p<0,05$ )..... 64

**Figure 11** Graph depicting the results obtained from  $^2\text{H}$ -enrichment NMR analysis of position 6S of liver MAG. The statistical analysis performed in this case was One-way ANOVA of multiple comparisons with Tuckey's post-test, which indicates that the HF group is significantly different from the SC group ( $*p<0,05$ ), while the HS and HFHS conditions are statistically different from the HF condition ( $*p<0,05$ )..... 65

**Figure 12** Graph depicting the results of the  $^2\text{H}$ -enrichment NMR analysis of position 5 of liver MAG. The statistical analysis performed in this case was Kruskal-Wallis test of multiple comparison with Dunn's post-test, which indicates that the HS and HFHS conditions are statistically different from the SC group ( $*p<0,05$ ) and the HS is also different from the HF group ( $*p<0,05$ )..... 66

**Figure 13** Panel of graphs summarizing Krebs cycle (KC) and the Triose phosphate (TP) contributions to the indirect pathway of glycogen synthesis. Graph A represents the results from the SC group, Graph B depicts the results obtained from the HF group, Graph C shows the results obtained from the HS condition, and Graph D depicts the results from the HFHS group The statistical analysis performed for Graph A consisted on a Mann-Whitney test, for Graph B and D consisted on an Unpaired T tests using the Welch correction and for Graph C was a standard unpaired T test. .... 67

**Figure 14** Graph depicting the fructose contribution to the indirect pathway of glycogen synthesis in HS and HFHS mice. The statistical analysis performed in this case was a Student's T test, reaching statistical significance ( $*p<0,05$ ). .... 68

**Figure 15** Graph describing the contributions of fructose to indirect pathway flux via the Krebs Cycle (left) and via triose phosphate (right) The statistical analysis performed on the left was a Mann-Whitney test, and on the right was a Student's T test..... 68

## Abbreviations

---

<b>ACC</b>	Acetyl-CoA carboxylase
<b>ALT</b>	Alanine transaminase
<b>AMPK</b>	Adenosine monophosphate-activated Protein Kinase
<b>aPKC</b>	Atypical Protein kinase C
<b>APOC3</b>	Apolipoprotein 3
<b>AST</b>	Aspartate Transaminase
<b>ATP</b>	Adenosine Triphosphate
<b>AUROC</b>	Area Under the Receiver Operating Characteristics
<b>BMI</b>	Body Mass Index
<b>BW</b>	<sup>2</sup> H-enriched Body Water
<b>C5</b>	MAG position 5
<b>C5D45</b>	[4,5- <sup>13</sup> C <sub>2</sub> ]glycogen
<b>C5D56</b>	[5,6- <sup>13</sup> C <sub>2</sub> ]glycogen
<b>C5Q456</b>	[4,5,6- <sup>13</sup> C <sub>3</sub> ]glycogen
<b>C5S</b>	<sup>13</sup> C-natural-abundance enrichment of carbon 5
<b>cAMP</b>	Cyclic Adenosine Monophosphate
<b>CNS</b>	Central Nervous System
<b>COVID-19</b>	Coronavirus Disease 2019
<b>DAG</b>	Diacylglycerol
<b>DGAT</b>	DAG acyltransferase
<b>DGAV</b>	Portuguese National Authority for Animal Health
<b>DHAP</b>	Dihydroxyacetone phosphate
<b>FABP4</b>	Fatty Acid Binding Protein 4
<b>FAS</b>	Fatty Acid Synthase
<b>FATP5</b>	Fatty Acid Transporter Protein 5
<b>FIB-4</b>	Fibrosis-4 Index
<b>FID</b>	Free Induction Decay
<b>FKH</b>	Forkhead Transcription factors
<b>FKHR</b>	Forkhead in rhabdomyosarcoma
<b>FructoseKC</b>	Contribution of exogenous fructose to total glycogen synthesis via Krebs cycle
<b>FructoseTP</b>	Contribution of exogenous fructose to total glycogen synthesis via Trioses Phosphate
<b>G3P</b>	Glyceraldehyde 3-phosphate

<b>G6Pase</b>	Glucose 6-phosphatase
<b>G6PT</b>	Glucose 6-phosphate Transporter
<b>GCK</b>	Glucokinase gene
<b>GGT</b>	$\gamma$ -Glutamyl Transferase
<b>GHS-R</b>	Growth Hormone Secretagogue Receptor
<b>GKRP</b>	Glucokinase Regulator Protein
<b>GLP</b>	Glucagon-like peptide
<b>GLUT</b>	Glucose Transporter
<b>GPAT</b>	Glycerol 3-phosphate Acyltransferase
<b>GSD-I</b>	Glycogen Storage Disease Type 1
<b>GSK3</b>	Glycogen Synthase Kinase 3
<b>HCC</b>	Hepatocellular Carcinoma
<b>HF</b>	High-Fat Diet
<b>HFCS</b>	High-fructose Corn Syrup
<b>HFHS</b>	High-Fat High-Sugar Diet (High-fat Diet + HFCS-55)
<b>HL</b>	Hepatic Lipase
<b>HS</b>	High-Sugar Diet (Standard Chow + HFCS-55)
<b>I/G</b>	Insulin/Glucagon
<b>ID</b>	Total Indirect Pathway of glycogen synthesis
<b>IDDM</b>	Insulin-dependent Diabetes Mellitus
<b>IDKC</b>	Krebs Cycle contribution to the Indirect Pathway of glycogen synthesis
<b>IDTP</b>	Triose phosphate contribution to the Indirect Pathway of glycogen synthesis
<b>IGF</b>	Insulin-like Growth Factor
<b>Ind KC from fructose</b>	Exogenous fructose contribution to the Krebs cycle component of the Indirect Pathway
<b>Ind TP from fructose</b>	Exogenous fructose contribution to the Trioses phosphate component of the Indirect Pathway
<b>Ip</b>	Intraperitoneal
<b>IRE</b>	Insulin Response Element
<b>Irs</b>	Insulin Receptor Substrate
<b>KHK</b>	Ketohexokinase
<b>KO</b>	Knockout
<b>LPL</b>	Lipoprotein Lipase
<b>MAG</b>	Monoacetone glucose

<b>MC4R</b>	Melanocortin 4 Receptor
<b>MCD</b>	Methionine and Choline deficiency
<b>MODY2</b>	Maturity Onset Diabetes Mellitus of the Young Type 2
<b>MRE</b>	Magnetic Resonance Elastography
<b>MRS</b>	Magnetic Resonance Spectroscopy
<b>MS</b>	Mass spectrometry
<b>MTBE</b>	Methyl Tert-Butyl Ether
<b>MTTP</b>	Microsomal Triglyceride Transfer Protein
<b>NAFL</b>	Non-Alcoholic Fatty Liver
<b>NAFLD</b>	Non-Alcoholic Fatty Liver Disease
<b>NAS</b>	NAFLD Activity Score
<b>NASH</b>	Non-Alcoholic Steatohepatitis
<b>NFS</b>	NAFLD Fibrosis Score
<b>NMR</b>	Nuclear Magnetic Resonance
<b>ORBEA</b>	University of Coimbra Ethics Committee on Animal Studies
<b>PDH</b>	Pyruvate dehydrogenase
<b>PDK1</b>	3-phosphoinositide-dependent protein kinase 1
<b>PEPCK</b>	Phosphoenolpyruvate carboxykinase
<b>PFK-1</b>	Phosphofructokinase-1
<b>PGC-1</b>	Peroxisome Proliferator-activated Receptor
<b>PI3K</b>	Phosphatidylinositol 3-kinase
<b>PIP2</b>	Phosphatidylinositol 4,5-bisphosphate
<b>PIP3</b>	Phosphatidylinositol 3,4,5-triphosphate
<b>PKA</b>	Protein Kinase A
<b>PKB/Akt</b>	Protein Kinase B
<b>PKC</b>	Protein Kinase C
<b>PKC-ε</b>	Protein Kinase C ε
<b>PLA2</b>	Phospholipase A2
<b>PLC</b>	Phospholipase C
<b>PNAPL3</b>	Patatin-like Phospholipase domain-containing protein 3
<b>PP1</b>	Protein Phosphatase 1
<b>PP1G</b>	Glycogen-associated Protein Kinase 1
<b>PTEN</b>	Phosphatase and Tensin Homolog
<b>Ptg</b>	Protein Targeting Glycogen
<b>RBP-4</b>	Retinol Binding Protein-4
<b>SAF</b>	Steatosis Activity Fibrosis Score

<b>SC</b>	Standard Chow
<b>SRE</b>	Sterol Regulatory Element
<b>SREBP</b>	Sterol Regulatory Element-Binding Protein
<b>T2DM</b>	Type 2 Diabetes Mellitus
<b>TG</b>	Triglyceride
<b>TLR-4</b>	Toll-like Receptor 4
<b>TNF</b>	Tumour Necrosis Factor
<b>UDP-Glucose</b>	Uridine Diphosphate Glucose
<b>VCTE</b>	Vibration-Controlled Transient Elastography
<b>VLDL</b>	Very Low-Density Lipoprotein

## Abstract

---

Non-alcoholic fatty liver disease (NAFLD) is considered to be the hepatic manifestation of the metabolic syndrome. In 2018, approximately 25% of the worldwide population was estimated to suffer from NAFLD and the incidence rates are expected to continue growing. Although the prevalence of NAFLD worldwide is rapidly increasing, routine screening is currently not practised even for high risk populations due to high costs and relative risks associated with the available diagnosis. There is no pharmacological treatment approved for this patients, whose only therapeutic option is weight loss, through lifestyle interventions.

In this study, we describe data from mice provided with high-fat, high-HFCS-55 and high-fat + HFCS-55, the latter resembling the Western diet. Generally, these models result in the induction of moderate weight gain and a mild form of NAFLD. From the perspective of hepatic glycogen metabolism, these models perturb hepatic insulin actions to different degrees as well as altering the portfolio of glycogenic substrates. Therefore, in addition to altering hepatic lipid metabolism and triglyceride levels, they are expected to significantly modify hepatic glycogen synthesis fluxes.

Our results show that hepatic glycogen concentration is not necessarily affected by diet composition in the context of NAFLD. High-fat feeding increased the indirect pathway, whereas HFCS-55 supplementation increased the direct pathway contribution to glycogen synthesis. Moreover, in mice under high-fat feeding, HFCS-55 supplementation prevented the increase in the indirect pathway contribution observed in mice fed high-fat diet only, instead of causing an intermediate profile. In this way, even though high-fat high-sugar diets are more efficient in promoting the development of NAFLD, it is also apparent that HFCS-55 counteract the effects of high-fat feeding on direct pathway glycogen metabolism. We have confirmed that fructose enters the gluconeogenic pathway through the trioses phosphate equilibrium, but more importantly we have demonstrated that fructose is incorporated into glycogen via the indirect pathway, while at the same time stimulating glucose usage via the direct pathway.

**Keywords:** direct and indirect pathway of glycogen synthesis, gluconeogenesis, high-fructose corn syrup, insulin resistance, alcoholic fatty liver disease.



## Resumo

---

Fígado gordo não alcoólico é considerada a manifestação hepática da Síndrome Metabólica. Em 2018, era estimado que aproximadamente 25% da população mundial sofresse de fígado gordo não alcoólico e é esperado que a taxa de incidência continue a aumentar. Apesar da prevalência da doença a nível mundial estar a crescer rapidamente, o diagnóstico de rotina não é praticado atualmente, mesmo em populações de risco, derivado ao custo e ao relativo risco associados aos métodos de diagnóstico disponíveis. Não existem terapias farmacológicas aprovadas para os doentes, cuja única opção terapêutica consiste na perda de peso através intervenções no estilo de vida.

Neste estudo, descrevemos dados obtidos de murganhos sujeitos a dietas ricas em gordura, em HFCS-55 ou em gordura e HFCS-55, sendo que a última se assemelha à dieta Ocidental. Geralmente, estes modelos resultam na indução de ganho de peso moderado e no desenvolvimento de num fenótipo ligeiro de fígado gordo não alcoólico. Do ponto de vista do metabolismo de glicogénio hepático, estes modelos afetam a ação da insulina no fígado a diferentes níveis, bem como o portefólio de substratos glicogénicos. Desta forma, além de apresentarem alterações ao nível do metabolismo hepático de lípidos e dos níveis de triglicéridos, é esperado que estes modelos apresentem alterações significativas no fluxo através das vias de síntese de glicogénio no fígado.

Os nossos resultados demonstram que a concentração de glicogénio hepático não é necessariamente afetada pela composição da dieta no contexto de fígado gordo não alcoólico. A dieta rica em gordura estimulou a via indireta para a síntese de glicogénio, enquanto a suplementação com HFCS-55 estimulou a contribuição da via direta para a síntese de glicogénio. Além do mais, em murganhos sujeitos à dieta rica em gordura, a suplementação com HFCS-55 preveniu o aumento da contribuição da via indireta para a síntese de glicogénio observada nos animais sujeitos apenas à dieta rica em gordura, em lugar de causar um perfil intermédio. Desta forma, apesar de dietas ricas em gordura e açúcar serem mais eficientes na promoção do desenvolvimento de fígado gordo não alcoólico, é também aparente que o HFCS-55 contraria os efeitos da dieta rica em gordura na via direta do metabolismo de glicogénio. Confirmámos que a frutose entra na gluconeogénese através do equilíbrio das trioses fosfato, mas, mais importante que

isso, demonstrámos que a frutose é incorporada no glicogénio pela via indireta, enquanto estimula a utilização da glucose pela via direta para a síntese de glicogénio.

**Palavras-chave:** via direta e indireta da síntese de glicogénio, gluconeogénese, xarope de milho rico em frutose, resistência à insulina, fígado gordo não alcoólico.

# Introduction

---

## Non-Alcoholic Fatty Liver Disease

Non-alcoholic fatty liver disease is considered to be the hepatic manifestation of the metabolic syndrome. In 2018, approximately 25% of the worldwide population was estimated to suffer from NAFLD and the incidence rates are expected to continue growing.<sup>1</sup> In 2016, the highest prevalence was reported from South America (31%) and the Middle East (32%), whereas the lowest was registered in Africa (14%), evidencing that abundances of food and wealth are not entirely proportional to the incidence of the disease (Figure 1).<sup>2</sup>

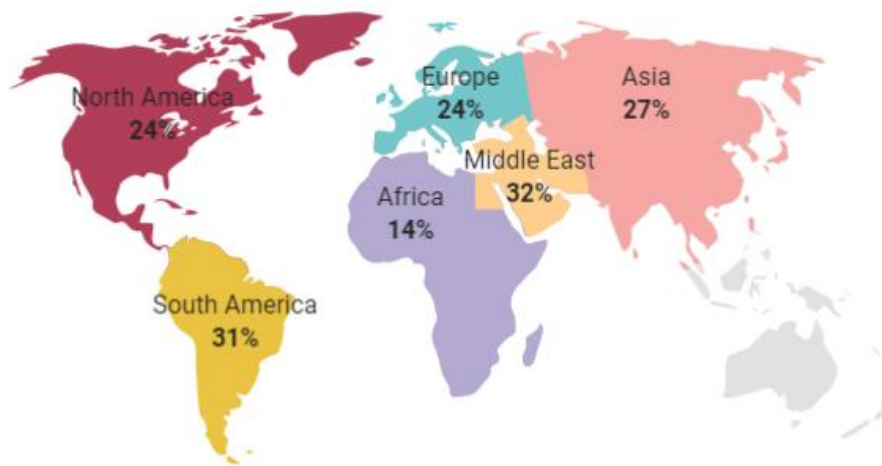


**Figure 1** World distribution of NAFLD patients adapted from Younossi, Z. et al. (2019). The highest incidence is registered in the Middle East and South America, followed by Asia, North America and Europe. The lowest incidence is verified in Africa.<sup>3</sup>

NAFLD is characterized by imbalanced triglyceride (TG) uptake and clearance, leading to excessive hepatic fat accumulation. Patients can be divided into two separate pathological groups: non-alcoholic fatty liver (NAFL) or simple steatosis and non-alcoholic steatohepatitis (NASH).<sup>4</sup> The percentage of patients developing NASH is also predicted to rise dramatically through 2030 due to an increasing elderly population, high intakes of fat and sugar, and a trend towards more sedentary lifestyles.<sup>5</sup>

NAFL is characterized by excess lipid accumulation in the liver in the absence of hepatocyte ballooning or fibrosis. NASH further entails lobular and portal inflammatory infiltration as well as hepatocyte ballooning with or without fibrosis. Fibrosis is a process where collagen is deposited within hepatic tissue by hepatic stellate cells. Therefore,

NASH is normally perceived as the progressive form of NAFL, even though recent reports evidence a small subset of NAFLD patients who developed liver failure, cirrhosis, hepatocellular carcinoma (HCC) and increased risk of cardiovascular disease without previously exhibiting NASH.<sup>1,3,4,6,7</sup> NASH evolution is also not linear, showing varying periods of progression, regression and stability, which are yet to be fully clarified (Figure 2).<sup>8</sup>

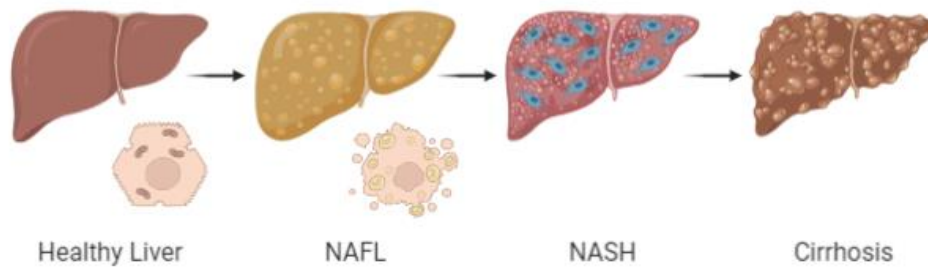


**Figure 2** Schematic illustrating disease progression. NAFL is characterized by triglyceride accumulation within lipid droplets and NASH by fibrosis and inflammatory infiltration. NASH patients can progress to cirrhosis and ultimately to HCC.

As a component of the metabolic syndrome, NAFLD has several associated comorbidities including obesity, insulin resistance, type 2 diabetes mellitus (T2DM) and cardiovascular disease. Even though the main risk factor for NAFLD is obesity, affecting 51% of NAFLD patients and 82% of NASH individuals, there is a significant fraction of patients who are not clinically overweight, whose body mass index (BMI) is below 27.<sup>2</sup> These show several metabolic dysfunction hallmarks, including insulin resistance and excess visceral adiposity. Interestingly, lean patients tend to be more predisposed to progress to NASH and therefore face higher rates of mortality.<sup>9</sup>

Several risk factors for NAFLD have been identified over the years, including age, sex, ethnicity, and some gene polymorphisms. However, the main causative effect is still attributed to lifestyle. Most patients are sedentary and have unbalanced diets.<sup>6,10</sup>

### *Diagnosis and prognosis*

Although the prevalence of NAFLD worldwide is rapidly increasing, routine screening is currently not practised even for high risk populations. This is due in part to the high costs and relative risks associated with its diagnosis.<sup>11</sup>

NAFLD is indicated by hepatic steatosis representing at least 5% of triglyceride by weight and/or macroscopic steatosis present in at least 5% of hepatocytes in the absence of secondary causes of liver damage, such as excessive alcohol intake, hepatitis C, Wilson's disease or hepatotoxic drugs. Diagnosis of liver fat content *per se* can be performed using several non-invasive imaging techniques including ultrasound, computed tomography and proton magnetic resonance spectroscopy (<sup>1</sup>H-MRS). Proton-MRS is currently the best technique to distinguish moderate/severe ( $\geq 33\%$ ) from mild steatosis ( $\geq 5\%$ ), with area under the receiver operating characteristic (AUROC) above 0,97.<sup>11-13</sup>

The classical circulating biochemical markers of liver damage are highly variable among NAFLD patients. As a consequence, no serological parameters are currently approved for diagnosis, but some can be used to evaluate the risk of disease progression, such as plasma concentrations of ferritin, alanine transaminase (ALT), aspartate transaminase (AST) and  $\gamma$ -glutamyl transferase (GGT). Additionally, there are also some helpful tools to evaluate the stage of disease, namely the NAFLD Fibrosis Score (NFS), the Fibrosis-4 (FIB-4) Index and liver stiffness measures performed by vibration-controlled transient elastography (VCTE) or magnetic resonance elastography (MRE).<sup>2,11,12,14,15</sup>

Proper diagnosis should further take into consideration the grade and stage of disease in order to distinguish between NAFL, NASH, borderline steatohepatitis and definite steatohepatitis. The grading is related to inflammation, while the staging is associated with fibrosis. The evaluation of fibrosis requires the performance of liver biopsy, which is a costly, and a highly invasive procedure, and has its own risks of morbidity and mortality. For these reasons liver biopsy is not performed unless there is strong evidence of advanced disease.<sup>11</sup>

In this way, NAFLD can be divided in NAFL (at least 5% steatosis, with or without lobular or portal inflammation), borderline NASH, zone 1 or 3 (steatosis accompanied by injury on zone 1 or 3, respectively, without meeting all the criteria for definite NASH) and definite NASH (steatosis, hepatocellular ballooning and lobular inflammation).<sup>16</sup>

There are 2 further scoring systems adequate for semiquantitative evaluation of necroinflammatory lesions: NAFLD Activity Score (NAS) and Steatosis Activity Fibrosis (SAF). Both of them require biopsies for histology staining.<sup>11,17,18</sup>

Long-term prognosis varies across the NAFLD spectrum. Patients who develop steatosis, but not considerable liver injury, may follow a relatively benign clinical course while NASH patients usually have increased rates of mortality. Fibrosis is a common feature among NAFLD patients and, although it is prevalent in NASH, it is not restricted to it. The stage of fibrosis (0 to 4) is highly correlated with all-cause and liver-associated mortality, making this parameter a highly important histological feature for prognosis. This relationship is independent of other histologic features, including the NAS score.<sup>19,20</sup>

### *Treatment*

The best current therapy available for all the spectrum of disease is weight loss, attained by hypocaloric diet and physical exercise. A 7% reduction in weight is sufficient for histological improvement, but this level of weight loss is achieved by less than 50% of the patients undergoing lifestyle interventions.<sup>21-26</sup> Moderate to vigorous physical activity can also prevent the development of NAFLD and decrease the propensity of patients to progress to NASH.<sup>27,28</sup>

There is no specific pharmacological treatment established for NAFLD. Usually, clinicians target liver disease and associated pathologies such as T2DM, obesity, hyperlipidaemia and/or insulin resistance.<sup>4,11</sup> Some authors also report improvements associated with vitamin E, omega-3 or ursodeoxycholic acid supplementation, but clinical trials show conflicting data.<sup>33-38</sup>

Bariatric surgery is commonly performed in patients with severe obesity and may represent a good weight loss strategy for those who struggle to follow strict diets and exercise regimens. Even though its efficacy and safety as a NAFLD therapy are still open for debate, several patients are eligible for gastric band, bilio-intestinal or gastric bypass and, consequently, have the surgery performed as a therapy for other comorbidities.<sup>11,35,36</sup>

## Endocrine and nutritional players in NAFLD

While the role of genetic polymorphisms, such as the patatin-like phospholipase domain-containing protein 3 (PNPLA3), are undoubtedly important determinants of NAFLD incidence and progression, this Thesis has focused on the role of high fat and/or

sugar feeding on hepatic intermediary metabolism in mouse models with a normal wild-type genetic background.<sup>37</sup> To this end, the focus will be on endocrine-nutrient-lipid interactions that can perturb hepatic intermediary metabolism in the NAFLD setting.

Insulin and glucagon are the two principal endocrine regulators of hepatic intermediary metabolism. Insulin is synthesized in the pancreatic  $\beta$ -cells, whereas glucagon is synthesized and stored in the  $\alpha$ -cells. These two hormones are regulated in a reciprocal manner by macronutrient intake and gastrointestinal hormones. Glucagon release is triggered by hypoglycaemia, while insulin is released in response to hyperglycaemia.<sup>38</sup>

### *The Insulin/Glucagon ratio*

Liver intermediary metabolism is highly directed by the so-called insulin/glucagon (I/G) ratio. A decrease in the I/G ratio promotes amino acid and fatty acid transport to the liver for gluconeogenesis; whereas an increase in the I/G ratio leads to glycogen synthesis in the liver and TG synthesis in adipose tissue.<sup>38</sup>

Portal and hepatovenous concentrations of insulin and glucagon are very different. For insulin, portal and hepatovenous concentrations are 1,6-1,9 nM and 0,4-1 nM, whereas for glucagon they are 50-80 pM and 30 pM, respectively. Hepatic glucagon extraction, in contrast to hepatic insulin extraction, is not significantly affected by food intake. In this way, the liver can modulate the I/G ratio in peripheral tissues by varying hepatic insulin extraction according to macronutrient abundance to guarantee appropriate management of substrate utilization and storage. Food intake decreases hepatic insulin extraction causing a rise in the peripheral I/G ratio that in turn promotes glucose uptake and catabolism. Brief fasting, in turn, causes an increase in hepatic insulin extraction to decrease the peripheral I/G ratio and as a consequence prevent peripheral tissues from exhausting the amount of available glucose and allow tissues that rely on glucose as their principal substrate, such as the central nervous system (CNS), to meet their energy needs.<sup>39</sup>

## *Insulin*

Insulin binds to its membrane receptor leading to its autophosphorylation and subsequent activation. The activated insulin receptor phosphorylates the insulin receptor substrate 1 and 2 (Irs1 and Irs2) molecules, which then associate with phosphatidylinositol 3-kinase (PI3K) causing its localization to the membrane. PI3K becomes active and phosphorylates the membrane phosphatidylinositol 4,5-bisphosphate (PIP2) yielding phosphatidylinositol 3,4,5-triphosphate (PIP3). A phosphatase enzyme called phosphatase and tensin homolog (PTEN) can remove the phosphate at position 3, inactivating phosphatidylinositol. PIP3 localizes 3-phosphoinositide-dependent protein kinase-1 (PDK1) to the membrane as well as some of PDK1's target molecules, including protein kinase B (PKB/Akt) and atypical protein kinase C (aPKC). PDK1 phosphorylates Akt and aPKC, causing their activation, which mediates many of insulin actions in metabolism. Irs1 and Irs2 are extensively expressed in the liver and are thought to modulate most of insulin signalling pathways. Irs1 in particular plays a dominant role under nutrient excess.<sup>40</sup>

In the liver, insulin and glucose act together to promote glycogen synthesis (glycogenesis). First, insulin decreases glycogen phosphorylase a activity to a level at which positive modulation of glycogen synthase by glucose becomes more effective, leading to glycogen synthesis. Insulin is incapable of activating either glycogen synthase or glycogen phosphorylase in isolated hepatocytes in the absence of glucose; thus glucose and insulin modulation of glycogen synthesis/degradation are interdependent.<sup>41,42</sup>

Hepatic protein phosphatase-1 (PP1) activates glycogen synthase leading to glycogen synthesis. Phosphorylase a inhibits PP1 through phosphorylation. After a meal, portal vein glucose concentration increases and is taken up by hepatocytes in a concentration-dependent manner. Once in the liver, glucose binds to phosphorylase a converting it to its less active form, phosphorylase b, and relieving the inhibition on PP1. PP1 causes the activation of glycogen synthase leading to glycogen synthesis.<sup>43,44</sup>

Glycogen synthase kinase 3 (GSK3) inhibits glycogen synthase activity via phosphorylation in basal conditions. Upon insulin stimulation, Akt becomes active and phosphorylates GSK3 at a serine residue that renders it inactive, causing the de-inhibition of glycogen synthase. In reverse, dephosphorylation of this serine residue by a phosphatase activates GSK3 to phosphorylate glycogen synthase to inhibit glycogen synthesis. Increased GSK3 activity has been associated with insulin resistance due to



reduced glucose clearance secondary to the inhibition of hepatic glycogen synthesis. Moreover, inhibition of GSK3 seems to promote insulin sensitization as well as diminished phosphoenolpyruvate carboxykinase (PEPCK) and glucose 6-phosphatase (G6Pase) expression in insulin resistant animals. In this way, GSK3 not only modulates glycogen synthesis but may also promote gluconeogenesis.<sup>43,44</sup>

## *Glucagon*

Glucagon and glucagon-like peptides 1 and 2 (GLP-1 and GLP-2) are encoded by the same proglucagon gene. Tissue-specific post-translational transformations lead to the expression of glucagon in pancreatic  $\alpha$ -cells and the expression of GLP-1 and GLP-2 in the brain and the intestine. The activities of this superfamily are exerted through the activation of highly specific G-coupled protein receptors.<sup>45</sup>

Glucagon can act on one of two G-coupled protein receptors:  $G_s$  or  $G_q$ . Binding and consequent activation of the  $G_s$  receptor activates adenylate cyclase leading to the increase in intracellular cyclic adenosine monophosphate (cAMP) concentration, which, in turn, activates protein kinase A (PKA) activity.<sup>46</sup> In the liver, PKA regulates PEPCK, G6Pase, fructose 1,6-bisphosphatase and peroxisome proliferator-activated receptor  $\gamma$  coactivator-1, causing downregulation of glycolysis and glycogen synthesis, and upregulation of gluconeogenesis and glycogen oxidation (glycogenolysis).<sup>47</sup>

Glucagon binding to the  $G_q$  receptor promotes the activation of phospholipase C (PLC) and increases diacylglycerol (DAG) levels with subsequent increase in calcium intracellular concentrations. In hepatocytes, the rise in calcium concentration is achieved by its release from intracellular stores and through extracellular influx. The increase in calcium concentration activates PKC and further stimulates glycogenolysis, gluconeogenesis and urea synthesis.<sup>47,48</sup>

Stimulation of glycogenolysis at the expense of glycogenesis is achieved by activation of glycogen phosphorylase and inhibition of glycogen synthase through phosphorylation of their regulatory enzymes in a cAMP-dependent pathway.  $G_s$  receptor activation also leads to decreased concentration of fructose 2,6-bisphosphate, an allosteric inhibitor of fructose 1,6-bisphosphatase and an activator of phosphofructokinase-1 (PFK-1), stimulating gluconeogenesis and inhibiting glycolysis. PKA activation also leads to inhibition of pyruvate kinase further inhibiting glycolysis. In

the adipose tissue, glucagon also promotes lipolysis leading to free fatty acid export to the liver.<sup>49–51</sup>

Oral glucose administration leads to more insulin release than intravenous glucose administration, due to gut secretion of incretins – the “incretin effect”. Incretins are a family of gastrointestinal proteins that potentiate insulin secretion from  $\beta$ -cells after food intake. These include GLP-1 and GLP-2.<sup>52</sup>

GLP-1 postprandial release to the splanchnic and portal circulations lowers plasma glucose by promoting insulin actions, while decreasing glucagon release and delaying gastric emptying. In NAFLD and NASH patients, glucose-induced GLP-1 release is impaired and is consequently associated with hyperinsulinemia and hyperglucagonemia. Even though GLP-1 impairment does not correlate with insulin resistance, glucose-induced GLP-1 secretion is decreased in patients with NAFLD/NASH. This indicates that GLP-1 signalling disruption might take place at early stages of NAFLD. Furthermore, GLP-1 administration decreases lipogenesis and increases fatty acid oxidation, thus ameliorating steatosis.<sup>53–55</sup>

GLP-2 is secreted in response to lipid and carbohydrate intake. It increases gastrointestinal absorption of carbohydrates via stimulation of their catalytic enzymes and transporters, and lipids through chylomicron secretion modulation. NAFLD/NASH patients have increased gut permeability as well as increased plasma endotoxin levels. Research shows that GLP-2 can ameliorate epithelial barrier function and improve inflammation in NAFLD/NASH patients. A protective role against dyslipidaemia and hepatic fat accumulation in high-fat diet mice has also been reported.<sup>56–58</sup>

### *Different roles of Irs1 and Irs2 in the insulin signalling cascade*

Insulin and insulin-like growth factors (IGFs) regulate several metabolic pathways via phosphorylation of the insulin receptor substrates, including Irs1, Irs2, Irs3 and Irs4. Humans do not express Irs3 and Irs4 is not expressed in the liver, therefore Irs3 and Irs4 are out of the scope of this dissertation.<sup>59</sup>

Forkhead transcription (FKH) factors localize to the nucleus and bind to the insulin response element (IRE) regions to counteract insulin action. During insulin signalling, Akt phosphorylates FKH forcing it to move to the cytosol. Nuclear exclusion of the forkhead in rhabdomyosarcoma protein (FKHR) leads to the inhibition of hepatic

gluconeogenesis and adipocyte differentiation as well as  $\beta$ -cell function improvement.<sup>59,60</sup>

Sterol Regulatory Element-Binding Proteins (SREBPs) are membrane-bound transcription factors capable of regulating the expression of several genes. Following cleavage, leucine zipper domains are translocated to the nucleus to bind to their sterol regulatory elements (SREs), leading to their target-gene promoters activation.<sup>61</sup> Different SREBP isoforms are responsible for regulating different pathways. For instance, SREBP-2 is involved in cholesterol synthesis, whereas SREBP-1c regulates lipogenic gene expression, including those encoding acetyl-CoA carboxylase (ACC) and fatty acid synthase (FAS). Therefore, SREBP-1c expression in hepatocytes and adipocytes is regulated by insulin and glucose availability.<sup>62,63</sup>

During fasting, FKH nuclear expression increases, causing its binding to the IRE region of the IRS2 promotor and concomitant IRS2 transcription. Carbohydrate refeeding reduces FKH nuclear expression, while increasing SREBP-1c concentration in the nucleus. SREBP-1c binds to SRE regions in the IRS2 promotor, causing its inhibition. In contrast, IRS1 transcription remains almost unaffected by the nutritional state, suggesting its regulation is independent from IRS2. SREBP-1c binding prevents FKHRL1 binding in a dose-dependent manner, even though they do not bind at the same site. Peroxisome proliferator-activated receptor 1 (PPAR-1) has been appointed as a transactivator of IRS2 transcription mediated by FKHS.<sup>64</sup>

In NAFLD patients, downregulation of *Irs2* is accompanied by upregulation of PEPCK and G6Pase leading to increased gluconeogenesis. Since IRS-1 signalling is conserved, patients demonstrate increased expression of SREBP-1c, which binds to the FAS promoter causing increased expression of FAS, hence promoting lipogenesis. In relation to NAFL, NASH is associated with higher elevation of FAS activity, even though increased activity of this enzyme is recurrent in all the spectrum of disease.<sup>65</sup>

Food intake activates insulin signalling pathways, including glycolysis and glycogen synthesis. PI3K/Akt activation leads to FKHS phosphorylation, removing these proteins from the nucleus. IRS2 expression is reduced and, as a consequence, PEPCK and G6Pase activity is decreased. In the meantime, nuclear expression of SREBP-1c increases, leading to lipogenic enzyme expression and reduced phosphorylation of serine 473 of Akt, stimulating lipogenesis and inhibiting glycogen synthesis, respectively. In the fully fed state, high concentrations of SREBP-1c and low concentrations of FKHS further inhibit IRS2 expression and insulin sensitivity.<sup>64</sup>

Both IRS1 and IRS2 knockouts (KOs) lead to decreased glycogen synthesis in mice. However, the effect caused by deletion of IRS2 is greater, suggesting that *Irs2* is responsible for coordinating glycogen synthesis.<sup>66</sup> In the liver, *Irs2* activation leads to Akt activation, which phosphorylates GSK3. GSK3 phosphorylation renders it inactive leading to dephosphorylation of glycogen synthase and subsequent upregulation of glycogen synthesis.<sup>67,68</sup>

## Insulin resistance in NAFLD

One of the first steps in the onset of NAFLD is disruption of insulin action leading to increased circulation of free fatty acids as well as hepatic TG synthesis and accumulation.<sup>69</sup> Circulating free fatty acids activate hepatic expression of SREBP-1c, leading to the expression of several lipogenic enzymes and consequently causing increased *de novo* lipogenesis. Activated SREBP-1c is also responsible for the inhibition of the microsomal triglyceride transfer protein (MTTP) expression, which lowers very low-density lipoprotein (VLDL) synthesis.<sup>70</sup>

Prolonged fatty acid deposition in the liver stimulates increased hepatic glucose output, causing increased plasma glucose levels (hyperglycaemia). Pancreatic  $\beta$ -cells respond by increasing insulin synthesis and secretion. Over time, the pancreas becomes incapable of maintaining the rate of insulin output necessary for euglycemia leading to glucose intolerance and diabetes.<sup>70</sup>

Insulin resistance is often associated with increased tumour necrosis factor  $\alpha$  (TNF- $\alpha$ ) and  $\beta$  (TNF- $\beta$ ), while adiponectin, ghrelin and leptin signalling are decreased. Adiponectin is known for promoting insulin sensitivity as well as preventing hepatic inflammation and fibrosis. Leptin is a sensor of adiposity and energy status. It binds to the hypothalamus leading to anorexigenic and thermogenic responses. It is also known to prevent ectopic deposition of triglycerides therefore preventing lipotoxicity. Ghrelin is an hormone secreted by the stomach which is responsible for mediating glucose and energy homeostasis. It also binds to the hypothalamus and antagonizes the effects of leptin. In humans, plasma ghrelin concentration is inversely related to body weight, especially body fat weight. In NAFLD insulin resistant patients, ghrelin levels are usually decreased.<sup>69</sup>

Fatty liver also secretes fetuin-A which impairs glucose-induced insulin secretion by the  $\beta$ -cells. Insulin secretion is further impaired by an inflammatory response caused by Toll-like receptor 4 (TLR4) activation that leads to macrophage infiltration of pancreatic tissue that in turn may contribute to the death of islet  $\beta$ -cells.<sup>71</sup>

### *Lipids as molecular drivers of insulin resistance*

Some lipid metabolites, including DAG, ceramide and acylcarnitine, have been proposed as molecular drivers of insulin resistance.<sup>63</sup>

Intrahepatic DAG accumulation caused by short-term high-fat feeding promotes translocation and activation of protein kinase C- $\epsilon$  (PKC- $\epsilon$ ), which phosphorylates threonine 1160 at the activation loop of insulin receptor kinase, leading to its inhibition. This occurs independently of increased adiposity or adipose tissue insulin resistance. Downregulation of PKC- $\epsilon$  expression prevents lipid-induced insulin resistance in the liver independently of hepatic TG and DAG levels. Thus, DAG accumulation and concomitant PKC- $\epsilon$  activation in hepatocytes are strong predictors of hepatic insulin resistance in obese adults, with no significant contributions derived from hepatic ceramides or inflammation.<sup>72–76</sup>

Ectopic lipid accumulation is regulated by hepatic expression of lipid transporters. Liver-specific overexpression of lipoprotein lipase (LPL) causes hepatic accumulation of DAG leading to hepatic insulin resistance.<sup>77</sup> Knockdown of fatty acid transport protein 5 (FATP5) protects mice from diet-induced hepatic steatosis and hyperglycaemia and can revert established NAFLD in a diet-induced obesity model. Furthermore, FATP5 overexpression in humans leads to insulin resistance.<sup>78</sup>

Visceral and intramyocellular fat deposition are important risk factors for insulin resistance in adolescence, independently of overall adipose tissue mass. In rats, surgical removal of the visceral fat depot leads to a massive decrease in insulin resistance, even though overall adiposity remains unchanged.<sup>79,80</sup> The rate at which free fatty acids are released from adipose tissue (lipolysis) decreases with increasing body fat. However, as adipose tissue grows, this compensation mechanism cannot avoid the increment in circulating free fatty acids, which are taken up by the liver, where they promote insulin resistance.<sup>81</sup>

Deletion of adipocytes' fatty acid binding protein 4 (FABP4), which preferentially binds long-chain fatty acids, improves insulin sensitivity and prevents the development of NAFLD in obese mice.<sup>82</sup> Moreover, deletion of adipocyte-specific phospholipase A2 (PLA2) in a leptin-deficient obesity mouse model increases lipolysis, causing ectopic lipid deposition and insulin resistance, even though animals remain lean.<sup>83</sup> FATP5 promoter polymorphism rs56225452 leads to a gain-of-function in this liver-specific fat transporter, which is associated with insulin resistance and dyslipidaemia, leading to severely steatotic livers in the course of NAFLD.<sup>84</sup>

Overexpression of apolipoprotein C3 (APOC3) in transgenic mice on standard chow increases hepatic TG uptake, which is compensated by increased VLDL production in the liver to avoid hepatic steatosis. High-fat feeding causes hyperinsulinemia, which prevents the production of VLDL. As a result, these animals' liver take up TG that they cannot export in VLDL particles, causing hepatic steatosis associated with hepatic insulin resistance in the same transgenic mouse model.<sup>85</sup> In humans, loss of function mutations affecting APOC3 correlate with reduced fasting and postprandial plasma TG concentrations. However, in obese humans with low visceral adiposity, APOC3 mRNA expression is associated with hepatic fat content.<sup>86</sup>

Morbidly obese subjects demonstrate increased hepatic lipase (HL) expression and activity compared to normal-weight individuals. Liver expression of this enzyme is driven by increased hepatic cholesterol content. HL activity correlates with insulin resistance, and weight loss results in a parallel decrease on these parameters. However, HL expression remains unchanged.<sup>87</sup>

Ectopic fat accumulation is increased when adipose tissue lipid deposition is impaired, promoting insulin resistance in liver and muscle. Mice expressing the dominant-negative protein A-ZIP/F-1 in adipocytes do not have visceral and peripheral fat depots, causing increased liver and muscle TG content and insulin resistance and affecting both Irs1 and Irs2 cascades. Transplantation of fat tissue into these mice decreases hepatic and muscle fat accumulation and improves insulin signalling in these tissues.<sup>88</sup> Lipodystrophy is a pathology characterized by selective loss of subcutaneous and visceral adipose tissue. Lipodystrophic patients demonstrate liver steatosis associated with hyperlipidaemia and severe hepatic insulin resistance. They also show increased rates of glycerol turnover, suggesting increased lipolysis in the remnant fat mass. Chronic leptin treatment decreases hepatic fat content and improves insulin signalling in muscle and liver.<sup>89</sup>

The majority of liver TG is formed by esterification of free fatty acids obtained from blood circulation with only a minor fraction derived from hepatic *de novo* lipogenesis. The reaction catalysed by mitochondrial glycerol 3-phosphate acyltransferase (GPAT) results in the esterification of a fatty acid to the *sn*1 position of glycerol 3-phosphate, and is the overall rate limiting step in TG esterification. Overexpression of GPAT1 causes increased PKC- $\epsilon$  activity leading to hepatic steatosis and insulin resistance in the absence of obesity or high-fat feeding.<sup>90,91</sup> Systemic deletion of GPAT1 prevents hepatic insulin resistance in mice under high-fat feeding, despite evidence of a large increase in hepatic long-chain and very long-chain acyl-CoA concentration.<sup>92</sup> Furthermore, inhibition of diacylglycerol acyltransferase 2 (DGAT2), the final enzyme in TG synthesis from DAG, causes decreased hepatic DAG content in response to downregulation of the lipogenic pathway. As a consequence, PKC- $\epsilon$  activity is increased, preventing the development of hepatic insulin resistance.<sup>93</sup>

In overnight-fasted rats, short-term elevation of free fatty acids causes increased activity of G6Pase leading to increased endogenous glucose production. Moreover, free fatty acids induce hepatic insulin resistance causing decreased activity of glucokinase, thus promoting net hepatic glucose output.<sup>94</sup>

### *Hepatic insulin resistance modulates $\beta$ -cell hyperplasia*

High-fat-induced insulin resistance triggers  $\beta$ -cell replication (hyperplasia) in order to increase insulin secretion and *Irs2* expression in wild-type mice. Glucokinase knockdown leads to insufficient hyperplasia upon high-fat intake, which is associated with lower expression of *Irs2*. Overexpression of *Irs2* increases hyperplasia, partially preventing diabetes. In this way, *Irs2* and glucokinase are important players in  $\beta$ -cell hyperplasia in response to diet-induced insulin resistance.<sup>95</sup> *Irs2* KO mice develop liver-specific insulin resistance, whereas *Irs1* KO mice exhibit insulin resistance in skeletal muscle. Moreover, deletion of *Irs2* leads to increased  $\beta$ -cell function, despite hyperplasia impairment, while *Irs1* deletion causes decreased  $\beta$ -cell function associated with hyperplasia.<sup>96</sup>

### *Paradoxes of hepatic insulin resistance, fatty acid oxidation and lipogenesis in NAFLD*

The initial stages of NAFLD are associated with insulin resistance, however NASH patients show more advanced impairment, characterized by lower rates of glycolysis and higher rates of  $\beta$ -oxidation compared to NAFL patients. Glycerol turnover, an indicator of whole body triglyceride lipolysis, is relatively unchanged across the NAFLD spectrum.<sup>97</sup>

As mentioned above, hepatic Irs1-mediated insulin signalling is conserved, despite Irs2-mediated insulin signalling impairment, therefore hepatic insulin resistance in the context of NAFLD is selective. Since lipogenesis is mainly regulated by Irs1, lipogenesis remains sensitive to insulin, even though gluconeogenesis and glycogen synthesis are insulin resistant due to Irs2-mediated signalling dysregulation.<sup>65</sup>

### The effect of diet composition in the obesity epidemic and the consequences for NAFLD – The threats of sugar and fructose

High-fructose syrups are produced from starch, which can be obtained from corn, rice, tapioca, wheat, cassava or sugar beet. Its production started in 1960 and dramatically increased over the past few years with favourable public reception. The most popular among them is high-fructose corn syrup (HFCS), whose biggest producer and consumer is the United States.<sup>98</sup>

HFCS can be found in all sorts of food products, including dairy, carbonated beverages, canned fruits, jams, jellies and baked goods.<sup>99</sup> HFCS-sweetened beverages, in particular, have been correlated with weight gain and the obesity epidemic in both short- and long-term studies.<sup>100</sup> Research shows that carbohydrate liquid intake is more deleterious than its solid consumption, reinforcing the danger of sugar-sweetened beverages, especially those using HFCS.<sup>101</sup>

The industry uses an isoform of glucose isomerase to increase the amount of fructose in corn-obtained syrups to intensify their sweetness, which leads to various formulations, which vary from 42 to 65 % fructose. HFCS-55 is the most popular in soft drinks and is roughly composed by 55% fructose and 45% glucose.<sup>99</sup> Given the prevalence of fructose in Western diets, there is now a renewed focus on its uptake and metabolism.



Fructose is directly absorbed across the small intestine border into enterocytes through glucose transporter 5 (GLUT5). In enterocytes, fructose is directly exported to the blood via GLUT2 and enters hepatocytes via GLUT2 or 5.<sup>102</sup> Even though the liver is considered to be the primary site of fructose metabolism, enterocytes also express the required enzymes and are thought to account for 10-30% of fructose utilization.<sup>103</sup>

Fructose metabolism could theoretically occur via two different pathways, one of them initiated by hexokinase and comparable to glycolysis, and the other initiated by an enzyme specific for fructose called fructokinase or ketohexokinase (KHK).<sup>104</sup> Hexokinase shows lower affinity for fructose than fructokinase *in vivo*, thus fructose catabolism is largely mediated via fructokinase.<sup>105</sup> This enzyme has two isoforms, KHK-A and KHK-C, which are differently expressed according to tissue. KHK-C is expressed primarily in the liver, kidney and intestine, whereas KHK-A is ubiquitously distributed.<sup>106</sup>

Even though KHK-A is able to metabolize fructose, its  $K_m$  is higher than KHK-C, which means that isoform C has higher affinity for fructose than isoform A. As a consequence, KHK-A is hypothesized to be involved in the phosphorylation of other carbohydrates. Furthermore, *in vitro* studies confirm that depletion of intracellular concentration of adenosine triphosphate (ATP) associated with KHK activity is lower for KHK-A, thus it is considered a slow metabolizer of fructose.<sup>107</sup> Fructose intake increases both KHK-A and KHK-C hepatic expression in wild-type mice. Moreover, KHK-A/C KO mice exposed to high-fructose intake become resistant to the metabolic syndrome. Yet, KHK-A deficient mice are more susceptible to this disease, probably because less fructose is catabolized in extrahepatic tissues where KHK-A may be more active.<sup>105</sup>

KHK mechanism involves the phosphorylation of fructose to fructose 1-phosphate. Unlike the phosphorylation of glucose, KHK activity is not regulated by insulin or by product inhibition, hence large inflows of fructose causes an acute decline in intracellular levels of ATP and concomitant rise in AMP. AMP is degraded by deaminases into purine products, including uric acid (Figure 3).<sup>108</sup>

Fructose 1-phosphate is subsequently metabolized to glyceraldehyde and dihydroxyacetone phosphate by Aldolase-B, with the glyceraldehyde converted to glyceraldehyde 3-phosphate by triokinase. The triose phosphate products can then be utilized for *de novo* lipogenesis or gluconeogenesis (Figure 3).<sup>103,109,110</sup>

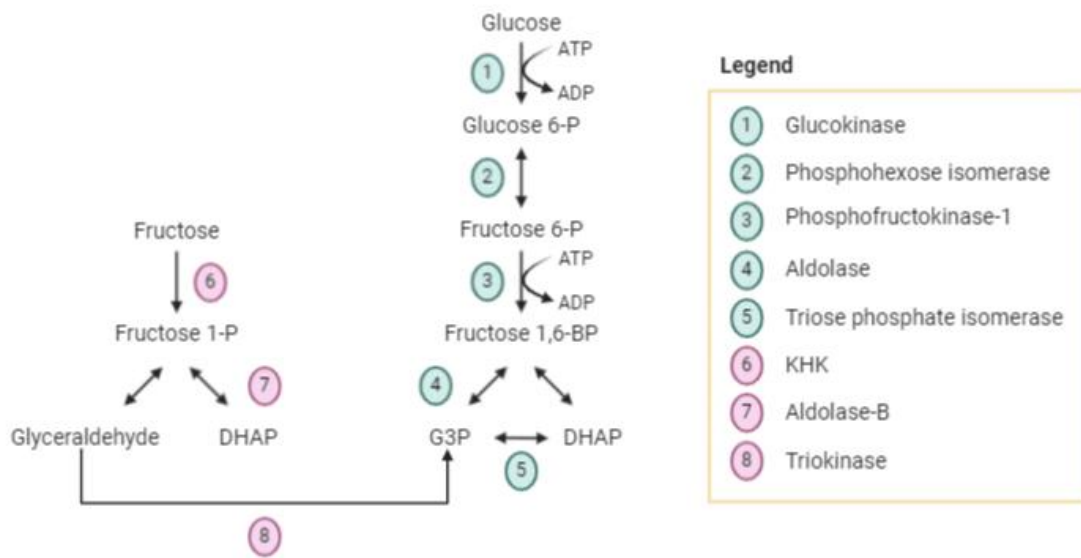


**Figure 3** Schematic representation of Glycolysis and Fructolysis, including the intervenient enzymes. The enzymes in blue belong to Glycolysis, while those in purple belong to Fructolysis.

Chronic high-fructose intake increases portal blood fructose concentration and consequent delivery to the liver, leading to hepatic metabolic derangements, such as increased hepatic *de novo* lipogenesis, inhibition of fatty acid  $\beta$ -oxidation, and reduced VLDL export.<sup>111–113</sup>

Fructose-sweetened beverages, including those with added HFCS, cause an acute increase of plasma triglycerides, in part due to increased *de novo* lipogenesis. Circulating triglycerides in turn decrease both insulin and leptin concentrations in peripheral tissues, causing impaired insulin and leptin responses.<sup>114–116</sup>

Fructose is more effective in promoting hyperinsulinemia and increased circulating TGs than either glucose or sucrose. HFCS in particular generates a circulating insulin and TG profile that is intermediate to that of pure fructose or pure glucose intakes. Interestingly, when evaluating the postprandial TG response, both sucrose and HFCS have a profile that is more similar to fructose compared to glucose.<sup>52</sup>

Besides causing decreased leptin synthesis in peripheral tissues, fructose intake also promotes leptin resistance, leading to a decline in satiety and consequent increase in calorie intake.<sup>105,118</sup> Interestingly, HFCS-55 causes a different response in terms of food intake. Mice supplemented with 10% sucrose (~5% fructose) in drinking water

adapt by taking fewer calories of chow, hence maintaining their body weight, while those having 8% HFCS-55 (~4,4% fructose) cannot adapt and become obese in 8 weeks.<sup>119</sup>

Fructose also causes a dose-dependent decrease in glycogen phosphorylase a activity, which is thought to be a consequence of allosteric inhibition of the enzyme by fructose 1-phosphate binding (one intermediate of Fructolysis). The half maximum inhibition in 2-hour refed livers after fructose perfusion can be attained with less than 1 mM of fructose, which means that the liver is very sensitive to fructose stimuli.<sup>120,121</sup>

A study conducted in overweight/obese above 40-year-old humans, showed that consuming a diet supplemented with 25% liquid fructose for 10 weeks, in opposition to glucose, causes increased production of GGT and retinol binding protein-4 (RBP-4). RBP-4 promotes increased hepatic glucose production through induction of PEPCK. Moreover, the subjects consuming fructose demonstrate visceral adipose tissue hyperplasia and associated adipose tissue insulin resistance, whereas those consuming glucose grow subcutaneous adipose.<sup>122</sup> One study also reported that fructose consumption increases the expression of GLUT5 and upregulates fructokinase activity in the liver in individuals with NAFLD.<sup>123</sup>

High-fat diets alone can promote obesity and NAFLD, through the development of hepatic insulin resistance, impaired insulin responsiveness and hyperinsulinemia. Nonetheless, the supplementation of the same diet with HFCS-55 further impairs insulin sensitivity and augments food intake, probably caused by leptin resistance.<sup>124</sup>

Fat-rich diets also promote fasting and postprandial lipoprotein elevations. Long-term high-fat feeding further causes higher amounts of fasting leptin concentrations as well as some NASH features, including portal inflammation and fibrosis. Moreover, lifestyle modification by replacement of the high-fat diet with a standard chow in a mouse model can improve hyperinsulinemia, insulin resistance, liver histology, inflammation and promote weight loss.<sup>40,125</sup>

Research comparing the effects of high-fat to high-fructose diets in rats, shows that even though both promote glucose intolerance and weight gain, high fructose intake is more successful in promoting insulin resistance and deleterious lipid profiles, without further weight gain or adiposity. Even though fat intake leads to more body and relative liver weight, only fructose can stimulate *de novo* lipogenesis leading to elevated plasma TGs and free fatty acids.<sup>126–128</sup> In a NAFLD mouse model liquid fructose/sucrose intake associated with a high-fat diet further promoted acute hyperphagia, epididymal adipose

tissue inflammation and hypertrophy as well as increased hepatic TG accumulation, weight gain and fibrosis.<sup>129</sup> Moreover, a study in a canine model proved that 13 week of high-fat high-fructose feeding led to impaired capacity of the liver to switch from glucose output to input, even in the presence of the portal glucose signal. These livers also showed decreased direct glycogen synthesis and a profile of glucose intolerance, characterized by hyperinsulinemia and hyperglycaemia.<sup>130</sup>

HFCS alone seems to promote an early stage of NAFLD, characterized by elevated fasting insulin and RBP-4 accompanied by decreased plasma adiponectin, suggesting a phenotype of insulin resistance and hepatic triglyceride accumulation. However, the absence of increased plasma triglycerides or free fatty acids in this mouse model indicates that even though 32 weeks of 20% HFCS-55 intake are not enough to cause advanced NAFLD, they can still promote an early stage of fatty liver disease.<sup>131</sup>

Furthermore, HFCS promotes adipose tissue inflammation and liver steatosis by a mechanism involving ghrelin and one of its receptors called growth hormone secretagogue receptor (GHS-R). GHS-R deletion decreases the ratio of pro-inflammatory to anti-inflammatory macrophages in adipose tissue, decreasing HFCS-mediated adipose tissue inflammation, liver steatosis and insulin resistance. In this way, ghrelin signalling might be at least partly responsible for increased risk of NAFLD caused by liquid HFCS intake in comparison to other diets.<sup>132</sup>

HFCS also causes decreased dopamine signalling in the absence of obesity or weight gain. Dopamine has been previously linked to compulsive eating (hyperphagia), decreased energy expenditure and impaired insulin function, all of which are hallmarks of the metabolic syndrome.<sup>133</sup>

In this way, we may conclude that HFCS-sweetened beverages present a threat to the liver. Their mechanism of action involves the disruption of several hormone-mediated signalling cascades, including insulin, leptin, ghrelin and dopamine. In the setting of NAFLD, these disturbances lead to decreased net hepatic glucose uptake but at the same time an increase in *de novo* lipogenesis. This latter factor contributes to TG accumulation as well as increased delivery of TGs to the bloodstream. It is also important to highlight the effects of HFCS on the central appetite/satiety signalling processes resulting in increased food intake thereby further flooding the liver with excess nutrients.

## Glycogen Metabolism

### *Importance*

The liver is responsible for balancing the concentrations of plasma carbohydrates, lipids and proteins, regardless of the nutritional intake. There are two ways of storing excess dietary glucose in mammals: glycogen and TGs.<sup>134</sup>

Glycogen is a very important energy short-term storage polymer in mammals. Hepatic glycogen stores serve the entire body and are usually mobilized in between meals or during a fast to guarantee that all tissues receive the fuels they need up to 12/24 hours of fasting. Therefore, the concentration of glycogen oscillates between 1 and 100 mg/g of liver tissue from fasting to feeding.<sup>135</sup> Glycogen is stored as granules in the cytosol of hepatocytes and muscle cells, which are composed of glycogen, its anabolic (glycogenesis) and catabolic (glycogenolysis) enzymes as well as some regulatory enzymes.<sup>135</sup>

### *Glycogenesis and the “Glucose Paradox”*

Glycogenesis is an ubiquitous pathway, taking place more extensively in the liver and skeletal muscle. The precursor for glycogen synthesis is glucose 6-phosphate, which can be derived from glucose via glucokinase in glycolysis or alternatively it can be synthesized via gluconeogenesis in the liver. These two sources have historically been referred to as the “direct” and “indirect” pathways of glycogen synthesis, respectively (Figure 4).

Glucose enters hepatocytes via GLUT2, whose activity is not regulated by insulin nor is the transport rate-limited by hepatic glucose uptake or release. As a result, the liver is sensitive to very small oscillations of glucose concentrations in the blood and the concentration of glucose in hepatocytes can be considered to be equivalent to that of the portal vein.<sup>136</sup>

Once glucose has entered the hepatocyte, it is phosphorylated by glucokinase to yield glucose 6-phosphate. The enzyme displays low affinity for glucose, due to its high  $K_m$ , yet glucose binding is competitive, leading to a sigmoidal saturation curve. A regulatory protein, whose activity is stimulated by fructose 6-phosphate and competitively antagonized by fructose 1-phosphate, negatively regulates the activity of glucokinase in the liver. In the presence of 1 mM fructose 1-phosphate, the activity of

glucokinase doubles in rat liver extracts.<sup>137,138</sup> Glucokinase regulatory protein (GKRP) regulates glucokinase localization in the cell. When glucose cytosolic concentration is low, GKRP binds glucokinase in the nucleus, inhibiting glucose phosphorylation. Glucose promotes glucokinase dissociation from GKRP, allowing its translocation to the cytosol, where it becomes active. Insulin mediates this glucose induced dissociation and also upregulates glucokinase expression via Akt. In contrast, glucagon inhibits this dissociation as well as glucokinase expression (Figure 4).<sup>139</sup>

Glucose 6-phosphate is isomerized to glucose 1-phosphate by phosphoglucomutase. The product is used by uridine diphosphate glucose (UDP-glucose) pyrophosphorylase to generate UDP-glucose (Figure 4).<sup>140,141</sup>

Glycogen synthase catalyses the addition of UDP-glucose to the nonreducing end of a nascent glycogen chain (Figure 4). The enzyme has two conformations: a and b. Both conformations catalyse glucose phosphorylation, but the activity rate of the b conformation is so low *in vivo* that it can be assumed that only the a conformation is active. Glycogen synthase conformation is regulated by phosphorylation. Many enzymes catalyse the phosphorylation of glycogen synthase at several residues inducing conformation change.<sup>142</sup> PKA and AMP-activated protein kinase (AMPK) promote phosphorylation of serine 7, which stabilizes conformation b. A serine to alanine substitution at this position causes increased hepatic glycogen deposition in both fasting and fed states. Mice with this mutation demonstrated improved glucose tolerance and decreased glycemia in the fed but not fasted state, emphasizing the role of glycogen synthesis in the fed condition.<sup>143–145</sup> Akt activation is essential for insulin-mediated GSK3-independent activation of glycogen synthase. Akt deletion leads to insulin resistance.<sup>146</sup>

Glucose 6-phosphate stimulates glycogen-associated protein phosphatase-1 (PP1G) to remove phosphate groups from glycogen synthase, causing its activation, in an insulin-dependent manner. PP1G activity is inhibited by phosphorylase a expression.<sup>147,148</sup>

Glycogenin is the other essential enzyme for the synthesis of glycogen. This enzyme binds to the first glycosyl unit derived from UDP-glucose via a tyrosine residue, and further catalyses the addition of 5-6 other UDP-glucoses to form the initial glycogen chain. When the chain is 6-7 residues long, glycogen synthase can take over and continues its extension. Glycogen synthase is initially bound to glycogenin but dissociates to begin elongation. Glycogenin is never detached from the first residue of glycogen, and remains bound to the single reducing end of the molecule.<sup>135</sup>

In 1983, Newgard and McGarry showed that only 12 to 28% of the glucosyl residues incorporated into glycogen could have been directly derived from glucose, regardless of the route of administration.<sup>149</sup> In a study where both glucose and fructose were intravenously administered to healthy human volunteers, the amount of hepatic glucosyl units derived from fructose was approximately four times higher than that obtained from glucose.<sup>150</sup> Additionally, the hepatic switch between glucose output to uptake following feeding was found to be determined in part by the portal vein glucose concentration. However, the postprandial portal vein glucose concentrations were deemed insufficient for generating the required amount of glucose 6-phosphate via glucokinase.<sup>151</sup> Thus, under physiological conditions, the liver was hypothesized to augment glycogenic glucose 6-phosphate production with gluconeogenic substrates.<sup>152</sup>

These observations were termed the “glucose paradox” by Katz and McGarry in 1984. It postulates that, although glucose is an important stimulator of hepatic glycogen synthesis, the majority of glycogen is synthesized from gluconeogenic precursors.<sup>153,154</sup> Formally, this can include glucose that is converted to pyruvate via glycolysis, which is then converted to glucose 6-phosphate via gluconeogenesis. At the time, there was widespread opposition to the concept of hepatic glycogen synthesis from any substrate other than glucose, hence the term “indirect pathway” was introduced, which refers to the conversion of glucose to glycogen via pyruvate and gluconeogenesis. Subsequently, it has been shown that gluconeogenic precursors that were not initially derived from glucose, such as fructose and gluconeogenic amino acids, can also feed the indirect pathway (Figure 4).<sup>155,156</sup>

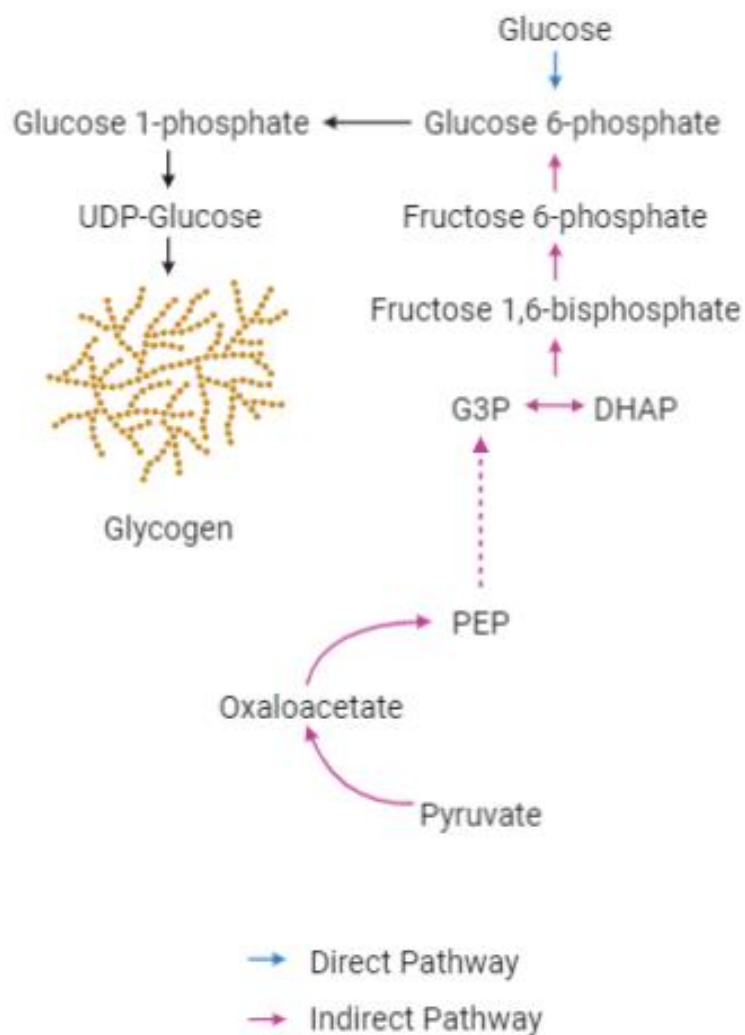


**Figure 4** Schematic representing the direct and indirect pathways of glycogen synthesis.

### *Glycogenolysis*

Glycogen oxidation is initiated by glycogen phosphorylase activity, which is also the rate limiting step of glycogenolysis. This enzyme promotes the cleavage of the ( $\alpha$ 1->4) glycosidic bond between two glycosyl units at a nonreducing end of glycogen. The reaction is a phosphorolysis, so each glycosyl unit is released as glucose 1-phosphate (Figure 5).



Glycogen phosphorylase is activated by conversion of its b to a conformation, which results from cAMP-PKA-mediated phosphorylation. The opposite conformational change promotes glycogen phosphorylase inhibition and is mediated by glucose 6-phosphate. Glycogen phosphorylase exists in two conformations: a and b. In line with glycogen synthase, both of these conformations are active, but only conformation a activity is high enough to promote phosphorolysis *in vivo*.<sup>157</sup> Moreover, PKA regulates both glycogen synthase and phosphorylase, leading to coordinated inhibition of the synthase and stimulation of the phosphorylase. This reciprocal regulation is mediated by protein-coupled receptor G<sub>L</sub>, which targets PP1. Glycogen phosphorylase a binds to PP1-G<sub>L</sub>, preventing PP1 activation and consequent dephosphorylation of glycogen synthase. In this way, PP1 prevents glycogen cycling. Moreover, glucose is an allosteric inhibitor of glycogen phosphorylase.<sup>158,159</sup>

Phosphoglucomutase catalyses the isomerization of glucose 1-phosphate into glucose 6-phosphate.<sup>141</sup> G6Pase removes the phosphate group from glucose 6-phosphate to yield glucose, which is exported to the bloodstream by GLUT2 (Figure 5). The only organs capable of expressing G6Pase are the liver and the kidney, thus they are the only ones in charge of preventing hypoglycaemia. Hyperglycaemia is associated with increased expression of G6Pase due to direct positive regulation by glucose even in insulin resistant diabetic mice.<sup>160,161</sup>

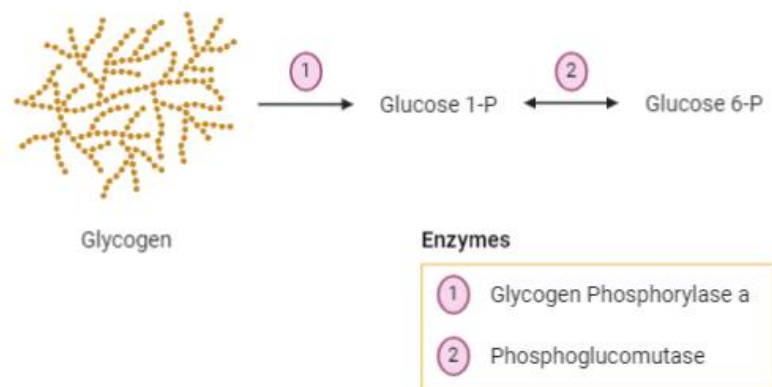


**Figure 5** Schematic representing the pathway of glycogen oxidation with the intervenient enzymes described.

The glycogen branching enzyme is responsible for catalysing the branching and debranching of the glycogen molecule. Although essential, it is not rate limiting for neither glycogenesis nor glycogenolysis. As a branching enzyme, it catalyses the transfer of a 6 to 7 glycosyl fragment from the nonreducing end of the nascent glycogen chain (having at least 11 glycosyl units) to the hydroxyl group at carbon 6 of a glucose at a more interior location of the same molecule. Branching conveys increased solubility and also increases the number of nonreducing ends. The last is critical for both glycogenesis and glycogenolysis, since glycogen synthase and glycogen phosphorylase can only act upon nonreducing ends.<sup>135</sup> As a debranching enzyme, it catalyses the transfer of a 4-unit fragment (from a 5-unit remaining branch) to a nearby branch to generate a linear chain at which glycogen phosphorylase can act. The remaining glycosyl unit attached to glycogen via a ( $\alpha$ 1->6) glycosidic bond is released by the branching enzyme instead of glycogen phosphorylase, because the latter cannot oxidize that bond. Glycogen phosphorylase and the debranching enzyme can also remove the last residue of glycogen from glycogenin via phosphorolysis of the last ( $\alpha$ 1->4) glycosidic bond and hydrolysis of the  $\alpha$ -glycosidic glucose glycogenin bond, respectively.<sup>135,162</sup>

### *Glycogen synthase and Glycogen phosphorylase interdependency*

Glycogen synthase and glycogen phosphorylase are the rate limiting enzymes of glycogenesis and glycogenolysis. Phosphorylase a is a strong inhibitor of glycogen synthase. Hepatic glucose uptake leads to increased glucose concentration in hepatocytes. There, glucose binds to phosphorylase a, priming it for the action of phosphorylase a phosphatase. In this way, phosphorylase a is converted to b and the synthase phosphatase becomes active. Synthase phosphatase removes the phosphate group from glycogen synthase leading to the conversion of glycogen phosphatase b into a, which can promote glycogen synthesis.<sup>163</sup>

### *Glycogen cycling*

Glycogen cycling is characterized by simultaneous activation of glycogen synthase and phosphorylase. Following a fast, glycogen cycling occurs mostly in the first few hours after a glucose load. It is hypothesized that this futile cycle is a consequence of the time required for body adaptation from fasted to fed states.<sup>164</sup> Moreover, glycogen

cycling may be a regulatory mechanism that allows glycogenolysis to be regulated by glycogen concentration in the fed state at which glycogen synthase is stimulated.<sup>165</sup>

In T2DM, glycogen cycling is increased, causing decreased glycogen stores in the liver. Overnight fasted patients demonstrate that at least 40% of their overall glucose production is derived from glycogen cycling, which is consistent with their low glycogen stores.<sup>166</sup>

## Glycogen Metabolism and Endocrine Control dysregulation

### *Glycogen storage disease type I (GSD-I)*

Glycogen storage disease type I or Gierke disease is a group of autosomal disorders that can be divided in GSD-Ia, caused by a deficiency in G6Pase, and GSD-Ib, characterized by a deficiency of glucose-6-phosphate transporter (G6PT). G6Pase and G6PT are necessary for the oxidation of glucose 6-phosphate to glucose, which is a shared step between gluconeogenesis and glycogenolysis in the liver. Recent data demonstrates that this two proteins are accountable for interprandial glucose homeostasis. Moreover, GSD-I patients demonstrate increased cytoplasmic glucose 6-phosphate concentration associated with increased hepatic glycogen deposition, as well as increased hepatic accumulation of neutral lipids, including cholesterol and TGs. Those are hallmarks of peripheral insulin resistance and, in fact, most of these patients develop NASH, which may progress to liver cirrhosis, hepatic adenomas and hepatomas.<sup>167</sup>

### *Maturity onset diabetes mellitus of the young type 2 (MODY2)*

Maturity onset diabetes mellitus of the young type 2 is a non-insulin-dependent variation of diabetes mellitus, which results from mutation in the glucokinase gene in chromosome 7. According to nature and position of the mutation in the gene, the phenotype changes from zero to low enzymatic activity and may also encompass decreased affinity for glucose. These patients demonstrate reduced glycogen accumulation in the liver throughout the day, independent of insulin expression and also show hyperglycaemia. Furthermore, the indirect pathway contribution is increased compared to control subjects and it is possible that glycogen cycling is also increased.<sup>168</sup>

### *Insulin-dependent diabetes mellitus (IDDM)*

Glycogen stores are essential to maintain euglycemia. Hepatic stores peak approximately 4 to 5 hours after each meal and rises gradually throughout the day. Since humans usually eat within less than 5 hours, the rate of glycogenolysis during the day is very low and this pathway becomes more essential to prevent hypoglycaemia during the night. In this way, during the day, plasma glucose is mostly obtained from gluconeogenesis or directly from meals.<sup>169</sup>

In IDDM, hepatic glycogenesis is depleted. Patients synthesize less than one third of the glycogen produced by healthy subjects in a day. The indirect pathway contribution for glycogen synthesis is also increased reaching 60% of glycogen synthesis following breakfast compared to only 35% registered in controls. It is hypothesized that this is the result of decreased glucokinase activity, which would impair the synthesis of glucose 6-phosphate, and/ or increase glycogen cycling following meals. Therefore, hepatic glycogen stores would be depleted. Nevertheless, the contribution of the direct pathway increases during the day for both sick and healthy subjects, suggesting that this pathway can be induced overtime even in the context of IDDM.<sup>169</sup>

### *NAFLD*

Even though it is widely accepted that glycogen synthesis is impaired in NAFLD, data regarding the impact of glycogen metabolism on the development of NAFLD is scarce. Most authors consider reduced hepatic glycogen content a manifestation of the disease.<sup>170,171</sup> Most of the information regarding the impact of hepatic glycogen stores in the course of NAFLD is derived from glycogen storage disease patients. The elevated incidence of NAFLD in patients of GSD highly suggests that glycogen metabolism impairment might be a risk factor for the development of NAFLD. GSDs are characterized by hypoglycaemia and increased liver size (hepatomegaly) and the most common phenotype among NAFLD patients is GSD-I, which has been discussed above.<sup>172</sup>

## Possible role of hepatic glycogen in the neuroendocrine regulation of food intake – The liver-brain axis

Insulin can cross the blood brain barrier and reach insulin receptors that are widely expressed in the brain, especially in the olfactory bulb, hypothalamus, cerebral cortex, cerebellum and hippocampus, even though its main target in the CNS is the hypothalamus.<sup>173,174</sup>

Insulin signalling in the brain promotes anorexigenic responses (i.e. decreased food intake).<sup>175</sup> Insulin signalling inhibition leads to an orexigenic response (i.e. increased food intake) and consequent weight gain associated with peripheral insulin resistance and hyperphagia.<sup>176</sup> Moreover, insulin activity in the brain activates mesolimbic dopaminergic neurons, independently of the anorexigenic response. These neurons are involved in mechanism of motivation, reward and reinforcing properties of natural stimuli, including food. Central administration of insulin specifically mediates glucose sensitivity in the liver and not the skeletal muscle.<sup>177</sup>

There are two types of glucose-sensing neurons: glucose-responsive and glucose-sensitive. The increase in glucose concentration in the interstitial fluid leads to increased firing of glucose-responsive neurons, but decreased firing of glucose-sensitive neurons. Glucose-responsive neurons use ATP-sensitive K<sup>+</sup> channels, which firing inhibition causes hepatic glucose synthesis impairment.<sup>178</sup>

In 1953, Mayer proposed the glucostatic theory of food intake, which establishes that blood glucose variation as a result of carbohydrate metabolism is the main regulator of hunger and satiety.<sup>179</sup>

In 1963, Russek proposed the hepatostatic theory which adds that the differences in glucose concentration in the portal vein promote an hepatic electric response that is sent to the hypothalamus to modulate food intake.<sup>180</sup>

In 1983, Langhans et al. proposed that it would be an hepatic polymer varying according to portal glucose concentrations that would cause the activation of neural glucose receptors in the liver that would mediate satiety. Interestingly, this author also showed that glycogenolysis would lead to a 25% decrease in glycogen content during meals, especially after fasting.<sup>181</sup> In 1996, Flatt further supported this evidence and proposed the glycogenostatic model suggesting that increased food availability in modern societies was causing increased deposition of glycogen in the liver, which would send electric signals to the hypothalamus leading to increased calorie intake.<sup>182</sup>

Furthermore, in 2015, Lopez-Soldado et al. demonstrated that increased hepatic glycogen content causes reduced food intake conveying protection against high-fat diet-induced obesity.<sup>183</sup> More recently, the same authors showed that hepatic branch vagotomy prevents the effect of glycogen deposition in the liver upon food intake. These mice accumulated more glycogen in the liver due to overexpression of protein targeting to glycogen (Ptg) but did not increase their food intake or develop glucose intolerance upon high-fat feeding. Moreover, vagotomy caused improved insulin sensitivity upon high-fat feeding, thus preventing insulin resistance. Controls oxidized more glucose, suggesting that the hepatic vagus nerve is involved in the regulation of carbohydrate oxidative pathways, besides food intake.<sup>184</sup> Another study published in 2016 by Winnick et al. further supports that liver glycogen regulates glycogen mobilization and hepatic glucose output in response to insulin-induced hypoglycaemia in a mechanism mediated by glucagon and epinephrine secretion as a result of liver innervation.<sup>185</sup>

## Methods for measuring total glycogen synthesis and hydrolysis rates

Hepatic intermediary metabolism comprises several catabolic and anabolic reactions that involve the entry of substrate precursors and the exit of end-products. The mechanisms involved in these, which include glycogen synthesis and oxidation, can be monitored using metabolic tracers. Metabolic tracers are compounds used to assess biological reactions involving endogenous substrates (tracées). The tracer must be chemically identical to the tracee so that it undergoes the same reactions but must also show a unique property that allows its detection unequivocally. Usually, tracers are man-made substrates at which one or more of the atoms has been substituted by an atom of the same chemical element, but of a different isotope (isotopic tracers). Isotopic tracers activity can be measured using radioactivity-based techniques, mass distance or nuclear spin variation.<sup>186</sup>

There are two isotopes commonly used for assessing glycogen synthesis: tritium and carbon-14. They have been widely used in scintillation counting procedures, since they are easy to detect, and their background radioactivity is low compared to metabolite specific activity. This technique is based on radioactive decay. Biological samples are mixed with a scintillator and  $\alpha/\beta$  photon emission (which is proportional to incorporation) is measured.  $^3\text{H}$  and  $^{14}\text{C}$  are commonly used scintillators in human and animal studies, because they are weak  $\alpha/\beta$  emitters, which makes them easily contained and allows for

high maximum permissible dosages. However, they are almost only used in cell culture studies nowadays, because radiation containment measures are more easily applicable in small scale studies.<sup>154,187</sup>

Stable isotope tracers have become more popular in recent years, especially for facilitating positional analysis. Nuclear Magnetic Resonance (NMR) spectroscopy and Mass spectrometry (MS) are the main techniques using stable isotope analysis. In both, the most widely used isotopes are deuterium and carbon-13, and molecules incorporating these tracers are usually called isotopomers.<sup>155,156,188</sup>

NMR spectroscopy is based on the interaction of electromagnetic radiation with matter. The intensity and shape of the peaks depend on the nature of the magnetic nuclei, the characteristics of the electric environment they are inserted into and the intramolecular relationships between them. NMR spectra are represented as graphs of probability of absorption/emission in function of frequency.<sup>189</sup>

MS consists on bombarding a sample with electron radiation leading to its breakage into charged fragments. These fragments are then separated according to their mass-to-charge ratio. MS spectra are graphs of intensity of detected ions in function of the mass-to-charge ratio.<sup>190</sup>

Depending on the positions at which the incorporation took place, these techniques provide information regarding the total synthesis of glycogen, but also the precursors that were used as substrates for that synthesis. Moreover, depending on the distance to the last meal, they provide information concerning the pre- and post-prandial state. They can be performed *in vivo* in both humans and animal models. Human samples are collected from biopsies, whereas in animals, the tissues are usually collected after euthanization and stored in liquid nitrogen.

## Animal models to study NAFLD

Animal models should be as close as possible to the human phenotype of disease. In the case of NAFLD that includes liver histology and pathology features. NAFLD comprises a wide spectrum of disease from simple steatosis to NASH, but the model should at least show 5% steatosis as well as some metabolic syndrome features such as insulin resistance, fasting hyperglycaemia, dyslipidaemia and disrupted

adipokine profile. There are no perfect animal models to study any disease, therefore the decision on which model to use should be made concerning the aim of the study.<sup>191,192</sup>

### *Genetic models of NAFLD*

Overexpression of SREBP-1c in adipose tissue causes lipodystrophy and consequent development of insulin resistance and hyperinsulinemia. Even though the fat tissue size is decreased, liver steatosis develops in 8 days. Moreover, 20 weeks are enough to observe associated lobular inflammation and periventricular and pericellular fibrosis, even in standard chow. The disadvantage of this model is that these mice fat tissue size is decreased, whereas humans show increased fat tissue hyperplasia.<sup>193,194</sup>

*Ob/ob* mice are leptin-deficient due to a spontaneous mutation in the gene encoding this protein. Leptin is an important adipokine secreted by white adipose tissue, which acts upon the hypothalamus to generate the anorexigenic response. This model is characterized by hyperphagia, obesity, hyperglycaemia, insulin resistance and hyperinsulinemia. However, the *ob* mutation is rare in humans.<sup>195–197</sup>

*Db/Db* mice have a mutation in the gene encoding the high-affinity leptin receptor OB-R, instead of the leptin gene. In accordance, they express normal or increased amounts of leptin, but are resistant to leptin signalling. They are often obese, insulin resistant and develop macrovesicular hepatic steatosis.<sup>198,199</sup>

The advantage of these two models is that they replicate most of the features observed in the human metabolic syndrome, even though these mice cannot progress to NASH without further stimuli, which means their phenotype is different from the one observed in humans.<sup>192,199</sup>

The Agouti gene mutation model results from a heterozygous mutation in the agouti gene (KK-*A<sup>y</sup>/a*) leading to melanocortin loss and obesity associated with hyperphagia and impaired hypothalamic appetite suppression. Once again, these mice develop hepatic steatosis with obesity and insulin resistance but cannot progress to NASH without further stimuli.<sup>200,201</sup>

PTEN is a tumour suppressor gene, which encodes for a phosphatidylinositol-3,4,5-triphosphate 3-phosphatase, catalysing the oxidation of PIP3 to PIP2. PTEN is



involved in the downregulation of several enzymes of the insulin signalling cascade, including PI3K and Akt.<sup>202,203</sup>

Liver-specific PTEN-null mice, which are identified as *AlbCrePTEN<sup>flox/flox</sup>* mice, develop steatosis and hepatomegaly, suggestive of NAFL and may progress to NASH. However, these mice are hypersensitive to insulin and demonstrate improved glucose tolerance in opposition to human NAFLD patients.<sup>203,204</sup>

Melanocortin 4 receptor (MC4R) activation is involved in the hypothalamic control of food intake. Many mutations in the MC4R gene have been associated with early-stage obesity in humans. Mice with MC4R gene disruption develop late-onset obesity accompanied by hyperphagia, hyperinsulinemia and hyperglycaemia.<sup>205,206</sup>

### *Dietary models of NAFLD*

#### 1. Methionine and choline deficiency (MCD)

Methionine and choline are necessary for proper hepatic  $\beta$ -oxidation and VLDL secretion. As a consequence, mice subjected to MCD develop steatosis associated with oxidative stress and impaired cytokine and adipokine profiles. CD57BL/6 mice demonstrate traits of NASH in less than 16 weeks, which are reversible, but longer periods of time exposure lead to irreversible fibrosis. Among species, Wistar males are the rats developing more severe steatosis and C57BL/6 are the rodents who approximate more to the human histological profile of human NASH. The main disadvantage of this model is that rodents experience significant weight loss, low plasma glucose, insulin sensitivity and low insulin and leptin secretion, which is in contrast with the human phenotype.<sup>192,195,207,208</sup>

#### 2. High-fat diet

High-fat diets are very efficient at inducing NAFLD. Furthermore, increased calorie intake is one of the main risk factors for developing NAFLD in humans, thus it may be the best approximation to the human context. This model leads to different degrees of steatosis, inflammation and fibrosis, besides being dependent on rodent species and strains. Even though these might be seen as issues, especially due to heterogeneity in

each cohort and between studies, NAFLD and NASH also produce very variable profiles in human patients, further supporting this approach, despite not being the most convenient.<sup>192</sup>

Rats under high-fat feeding develop marked steatosis and oxidative stress, which can be reverse with dietary restriction. In C57BL/6J mice, chronic exposure to 60% fats in the diet *ad libitum* causes NASH, and intragastric overfeeding with 85% excess for 9 weeks replicates histopathology and pathogenesis of human NASH. These mice become obese, show increased visceral fat, hyperglycaemia, hyperinsulinemia, hyperleptinemia, glucose intolerance, insulin resistance, reduced adiponectin expression, neutrophil infiltration, fibrosis and elevated ALT.<sup>209,210</sup>

### 3. Cholesterol and cholate

A diet enriched with 1,25% cholesterol and 0,5% cholate has been shown to induce progressive steatosis, inflammation, fibrosis and oxidative stress in a time-dependent manner over 6-24 weeks. The addition of 60% cocoa butter accelerated the development of symptoms and exacerbated insulin resistance. Although the model demonstrates histological features of NASH, mice lose weight, do not increase fat deposition in fat pads and have low plasma TG concentration. In this way, the model is quite different from human NASH.<sup>211</sup>

### 4. Fructose

There is evidence that an increment in the amount of fructose in human diets is associated with the obesity epidemic. Therefore, it is highly probable that increase fructose ingestion leads to obesity-associated comorbidities, including NAFLD.

Wistar rats under 70% fructose intake develop significant macrovesicular steatosis, intralobular inflammation and increased liver to body weight ratios in only 5 weeks, even though triglycerides are mainly deposited in zone 1, whereas in humans they are at zone 3.<sup>212</sup> Wistar albino rats supplemented with 10% fructose in drinking water can develop macro- and microvesicular steatosis as well as oxidative stress after 10 days.<sup>213</sup> In mice, 30% supplementation in drinking water causes marked hepatic steatosis and increased weight over 8 weeks.<sup>214</sup>

## 5. Western Diet – High-fat high-sugar feeding

A food regimen rich in both fat and fructose with sometimes slightly increased amounts of cholesterol is often referred to as the Western diet, because it resembles the diets of inhabitants of Western countries. Furthermore, animals on a western diet progress to NASH more rapidly than those fed by high-fat or high-fructose diets, suggesting a synergistic effect of fat and sugar in the progression of the disease.<sup>191</sup>

C57BL/6 mice exposed to a diet with 40% fat and 2% cholesterol accompanied by HFCS supplementation in drinking water (42 g/L) become overweight, insulin resistant and show features of NASH with increased fibrosis after 6 months. They can also develop marked hepatic steatosis and inflammation. Moreover, a 12-week high-fat high-fructose diet seems to be enough to promote micro- and macrovesicular steatosis, even though they only accumulate significant amounts of TGs at week 16, further supporting the idea that insulin resistance and the NAFLD phenotype is driven by early-stage hepatic expression of diacylglycerols.<sup>215</sup>

## Objectives

---

In this study, we describe data from mice provided with high-fat , high-HFCS-55 and high-fat + HFCS-55, the latter resembling the Western diet. Generally, these models result in the induction of moderate weight gain and a mild form of NAFLD. Previous unpublished studies suggest that glucose tolerance and insulin sensitivity tend to be more compromised in the high-fat fed mice compared to high-sugar fed animals. The high-fat plus high-sugar mice are considered to show the largest weight gain, greatest loss of insulin sensitivity and the most advanced extent of NAFLD. From the perspective of hepatic glycogen metabolism, these models perturb hepatic insulin actions to different degrees as well as altering the portfolio of glycogenic substrates. Therefore, in addition to altering hepatic lipid metabolism and triglyceride levels, they are expected to significantly modify hepatic glycogen synthesis fluxes.

Characterizing the sources of hepatic glycogen synthesis in these settings with stable isotope tracers will provide additional valuable insights into how some of the principal fluxes of hepatic carbohydrate metabolism are altered by diet-induced NAFLD. Moreover, such insights can be directly translated into NAFLD patients through non-invasive sampling of tracer incorporation into glycogen precursors such as UDP-glucose.<sup>188,216–218</sup> A deeper insight of hepatic carbohydrate metabolism in NAFLD patients will, among other things, improve our understanding of how anti-hyperglycaemic medications such as Metformin or Pioglitazone act in ameliorating NAFLD. Also, they will improve our understanding of how an excess of dietary lipid and/or sugar influence the actions of the liver in glycaemic control.

In this way, our scientific questions for this project were:

1. Is the amount of glycogen synthesized in the liver of a NAFLD model affected by diet composition?
2. Is diet composition affecting the direct and indirect pathway contributions to glycogen synthesis in NAFLD?
3. Is fructose being used as substrate to glycogen synthesis in the context of NAFLD?

# Materials and Methods

## Reagents

All the reagents and supplies used during this study are described on Table 1, including the information concerning their purity grade, manufacturers/suppliers, reference and CAS number.

**Table 1** Detailed description of all the reagents employed in this project, including their suppliers.

Reagent	Purity grade	Supplier	Reference	CAS number	
<b>Glycogen extraction and purification</b>					
Potassium hydroxide (KOH)	85,7%	Fisher Scientific, UK	P/5640/60	1310-58-3	
Sodium sulphate (NA <sub>2</sub> SO <sub>4</sub> )	≥99%	Sigma-Aldrich	239313-500G	7757-82-6	
Ethanol	≥99%	Fisher Scientific, UK	E/0600DF/F21	64-17-5	
Hydrochloric acid (HCl)	37%	Sigma-Aldrich	320331-500ML	7647-01-0	
Methyl tert-butyl ether (MTBE)	≥99.8%	Sigma-Aldrich	34875-2.5L	1634-04-4	
Nitrogen (N <sub>2</sub> )					
<b>Glycogen digestion to glucose</b>					
Sodium acetate trihydrate	Acetate buffer	99%	Alfa Aesar	A16230	6131-90-4
Acetic acid	pH 4,8	≥99%	Alfa Aesar	33252	64-19-7
Hydrochloric acid (HCl)	37%	Sigma-Aldrich	320331-500ML	7647-01-0	
Potassium hydroxide	85,7%	Fisher Scientific, UK	9/5640/60	1310-58-3	
Amyloglucosidase from <i>Aspergillus niger</i>	59U/mg	Fluka biochemika	10115	9032-08-0	
<b>Glucose derivatisation to monoacetone glucose</b>					
Sulfuric Acid (H <sub>2</sub> SO <sub>4</sub> )	95-98%	Sigma-Aldrich	339741-100ML	7664-93-9	
Deuterated water ( <sup>2</sup> H <sub>2</sub> O)	Acetone, 2% D	99,8% D	Cortecnet	CD5251P1000	7789-20-0
Acetone		≥99,8%	Merck Millipore	1000142511	67-64-1

Sodium hydroxide (NaOH)		≥97%	Merck Millipore	1064621000	1310-73-2
Hydrochloric acid (HCl)		37%	Sigma-Aldrich	320331-500ML	7647-01-0
Drierite®		100%	Sigma-Aldrich	238937-454G	7778-18-9
[U- <sup>13</sup> C <sub>6</sub> ]Glucose		99% C	Cambridge Isotope Laboratories, Inc	CLM-1396-10	110187-42-3
Sulfuric acid-d <sub>2</sub>		99,5% D	Aldrich chemistry	176796-25G	13813-19-9
Sodium carbonate anhydrous (Na <sub>2</sub> CO <sub>3</sub> )		≥99%	Labkem	SOCA-00P-1K0	497-19-8
Ethyl acetate		99,97%	Fisher Scientific, UK	E/0900/FP21	141-78-6
<b>Monoacetone glucose purification</b>					
Acetonitrile		≥99,7%	Alfa Aesar	22927	75-05-8
Discovery® DSC-18 SPE Tube (wt. 500 mg, volume 3mL)		-	Sigma-Aldrich	52603-U	-
<b>NMR experiments</b>					
Acetonitrile		≥99,7%	Alfa Aesar	22927	75-05-8
Hexafluorobenzene		99%	Acros Organics	120545000	392-56-3
<b>Glycogen quantification</b>					
Amyloglucosidase from Aspergillus niger		59U/mg	Fluka biochemika	10115	9032-08-0
<b>Animal experiments</b>					
[U- <sup>13</sup> C <sub>6</sub> ]Fructose		99%	Omicron	FRU-0111	201595-65-5
Sodium Chloride (NaCl)		≥99%	M&B laboratory chemicals	K1840	7440-23-5

## Experimental models and management

The animal studies were approved by the University of Coimbra Ethics Committee on Animal Studies (ORBEA) and the Portuguese National Authority for Animal Health (DGAV, 0421/000/000/2013). All animal procedures were performed

according to DGAV guidelines as well as European regulations (European Union Directive 2010/63/EU).

This project featured 46 young adult male C57BL/6J mice purchased from Charles River Labs, Barcelona, Spain and housed at the University of Coimbra UC-Biotech Bioterium. They were accommodated in a well-ventilated room under a 12 hours light/12 hours dark cycle. Before the beginning of the experiment, mice were allowed to accommodate for 2 weeks with free access to both standard chow and water. Four mice were kept in each cage.

The study was conducted for 16 weeks, following the 2 weeks of accommodation. Half the mice were given standard chow 4RF21 (60% carbohydrate, 7% fat and 27% protein) and the other half were given one high-fat chow (25% carbohydrate, 54% fat and 21% protein). These chow cohorts were each subdivided into two groups, one of which where the drinking water was supplemented with 30% (w/v) of a 55/45 mixture of fructose and glucose, corresponding to HFCS-55, and the other where no additions were made to the drinking water. As a consequence, there were 4 groups, each corresponding to one type of diet: standard chow (SC), high-fat (HF), standard chow plus HFCS-55 (HS) and high-fat plus HFCS-55 (HFHS) as shown in Table 2. Mice were randomly allotted to each group.

At the beginning of the final evening, all animals were administered with 99%  $^2\text{H}_2\text{O}$  containing 0,9 mg/mL NaCl intraperitoneally to achieve a loading dose of ~4 g per 100 g of body weight. They also had their drinking water replaced with 5%  $^2\text{H}$ -enriched water. For the animals whose drinking water was supplemented with HFCS-55, this was replaced with HFCS-55 where the fructose component was enriched to 20% with [U- $^{13}\text{C}_6$ ]fructose. In the following morning, mice were deeply anesthetized with ketamine/xylazine and sacrificed by cardiac puncture. Arterial blood was collected and centrifuged to isolate plasma, livers were freeze-clamped, and the samples were stored at -80 °C until further processing.<sup>219</sup>

For logistical purposes, the full study cohort was divided into 3 batches with 4 animals per condition, resulting in 16 mice being followed together at the same time. There was also a 2-week interval between each batch resulting in the completion of the last cohort 52 weeks after the start of the first batch. Two animals, one from the HF and one from the HFHS group had to be euthanized during the course of the feeding trial hence they are not included in the final data.

**Table 2** Table describing the experimental conditions, including the number of animals involved as well as the diets assigned to them

Chow	Supplementation in drinking water	Name of the Diet	#
Standard	None	Standard Chow (SC)	12
	30% HFCS-55 (w/v)	High-Sugar (HS)	12
High fat	None	High-fat (HF)	11
	30% HFCS-55 (w/v)	High-fat high-sugar (HFHS)	11
			46

## Glycogen extraction, derivatization and purification to monoacetone glucose (MAG)

### 1. Glycogen extraction

Livers were finely ground under liquid nitrogen and lipids were extracted using the MTBE lipid extraction protocol and both the lipid extracts and the insoluble material containing the liver glycogen were stored at -80 °C.<sup>220</sup> The insoluble material was mixed with 30% KOH (2 mL/g of original liver tissue) at 70 °C. Once the material was completely dissolved, 6% sodium sulphate (1 ml/g of original liver weight) was added and the glycogen then precipitated with ethanol (7 ml/g of original liver weight). The samples were then centrifuged for 10 minutes at 3000 rpm and the supernatant was removed. The pellet was resuspended in 5 mL of water and the pH adjusted to 7-8 with hydrochloric acid and the samples were then lyophilized.<sup>216</sup>

### 2. Glycogen digestion to glucose

Samples were resuspended in acetate buffer (5 mM, pH 4,5). An initial aliquot of 100 µL was collected from each sample for liver glucose quantification. Each sample was incubated for 6 hours with 120 units of amyloglucosidase at 55 °C. They were then centrifuged for 10 min at 3500 rpm and the supernatant collected. A final 100 µL aliquot



was collected for glucose quantification following glycogen hydrolysis and the samples were then lyophilized.<sup>216</sup>

### 3. *Glucose derivatization to MAG*

Samples were mixed with 5 mL <sup>2</sup>H-enriched acetone containing sulphuric acid enriched to 2% with <sup>2</sup>H<sub>2</sub>SO<sub>4</sub> (4% v/v). The solution was stirred for 14 to 18 hours overnight at room temperature.<sup>216</sup> The reaction was quenched by adding 5 mL of water to each sample and the pH was adjusted to 2,2-2,3 using sodium carbonate. The samples were then incubated at 40 °C for 5 hours and their pH readjusted to 7-8 using sodium carbonate. Finally, they were lyophilized in a Genevac rotor. The following day, the dried material was extracted with 5 mL boiling ethyl acetate and the supernatant was removed and evaporated with a rotatory evaporator.<sup>221</sup>

### 4. *MAG purification*

A set of 500 mg DSC-18 SPE columns was washed with 3 mL of acetonitrile and 10 mL of water. Each sample was loaded in 1,5 mL of water in the column and the waste fraction was collected. Then, the columns were eluted with 2,5 mL of 10% acetonitrile/90% water v/v to collect the MAG fraction. The MAG fraction was left to dry in the fume hood overnight and lyophilized until further analysis.<sup>221</sup>

## Glycogen quantification

Hepatic glycogen quantification was performed using the initial and final aliquots from the glycogen hydrolysis protocol. These aliquots were assayed for glucose with a Cobas Miura S spectrophotometric analyser (Hoffman-La Roche, Switzerland) according to the protocol described by Keppler and Decker.<sup>222</sup> To assess the amount of glycosyl units in the glycogen molecule, the glucose measured in the initial aliquot was subtracted from that measured in the final aliquot. The molecular weight of the glucosyl unit was assumed to be 180,156 g/mol and glycogen concentrations were expressed as μmol of glycosyl units per gram of tissue wet weight.

## NMR experiments

### *Deuterium and Carbon-13 spectra acquisition parameters*

Proton-decoupled  $^2\text{H}$ -NMR spectra were acquired at 50 °C using a Bruker Avance III HD 500 MHz spectrometer with a  $^2\text{H}$ -selective 5 mm probe incorporating a  $^{19}\text{F}$ -lock channel. Samples were resuspended in 0,5 mL 90% acetonitrile/10%  $^2\text{H}$ -depleted water with 50  $\mu\text{L}$  of hexafluorobenzene added to obtain a  $^{19}\text{F}$  lock signal. A pulse angle of 90° and acquisition time of 1,2 sec followed by 0,1 sec of inter-pulse delay was used. Between 2 444 and 30 688 free-induction decays (FID) were obtained for each sample, which were then processed with 0.5 Hz line-broadening and zero-filled to 4096 points before Fourier transform.

To determine deuterium enrichment of the body water, 10  $\mu\text{L}$  plasma samples were analysed by  $^2\text{H}$ -NMR as previously described using 50  $\mu\text{L}$  of hexafluorobenzene.<sup>217</sup>

For MAG samples obtained from livers of mice fed HFCS-55 with [ $\text{U-}^{13}\text{C}$ ]fructose, after obtaining the  $^2\text{H}$ -NMR spectra they were evaporated and resuspended in 99.9%  $^2\text{H}_2\text{O}$  for acquisition of  $^{13}\text{C}$ -NMR spectra. Proton-decoupled  $^{13}\text{C}$ -NMR spectra were obtained at 25 °C with a Varian VNMRS 600 MHz spectrometer (Agilent, Santa Clara, California, USA) using a 3 mm broadband probe with z-gradient. A pulse angle of 60° and acquisition time of 4,0 sec acquisition time followed by 0,1 sec of pulse delay was used. The number of FID collected per sample ranged from 1 640-13 128. The summed FID was processed with 0,2 Hz line-broadening and zero-filled to 131 072 points before Fourier transform.

## Metabolic Flux evaluation

### *1. Glycogen deuterium enrichment*

Deuterium is an isotope of hydrogen which is detectable by NMR. Its natural abundance is 0,015%, meaning that enrichment of body water to 4% by the intraperitoneal (ip) injection represents a 267-fold excess over the background.<sup>223</sup> Therefore, in our experimental setting, we can assume that the contribution of background  $^2\text{H}$  to the  $^2\text{H}$ -enrichment of metabolic intermediates is negligible and that the observed  $^2\text{H}$ -enrichment distribution of glycogen reflects its biosynthesis during the overnight interval that the animal was administered with  $^2\text{H}$ -enriched water.

The MAG  $^2\text{H}$ -NMR spectrum is well resolved allowing the evaluation of each hydrogen position of the glucose units derived from glycogen digestion. In this study we were interested in assessing the balance between the direct and indirect pathways of glycogen synthesis, as well as the substrate precursors of the indirect pathway.

Indirect pathway contributions include all gluconeogenic precursors that pass via the Krebs cycle. These result in deuterium enrichment of position 5 as well as the position 6 hydrogens of glucose.<sup>224</sup> As indicated in Figure 6, the signals of the *R* and *S* hydrogens of position 6 are fully resolved. In this study, we decided to consider only enrichment of the 6*S* position, because it is derived by an obligatory addition of water hydrogen via the hydration of fumarate to malate, while enrichment of position 6*R* is conditional on the exchange of pyruvate methyl hydrogens with water which may be incomplete.<sup>218</sup>

Indirect pathway contributions from substrates that enter at the level of triose phosphates, which include glycerol and fructose, result in enrichment of glucose position 5 but not the position 6 hydrogens. Thus, the difference between 5 and 6*S* enrichments informs the contributions of these substrates to the indirect pathway.<sup>155</sup>

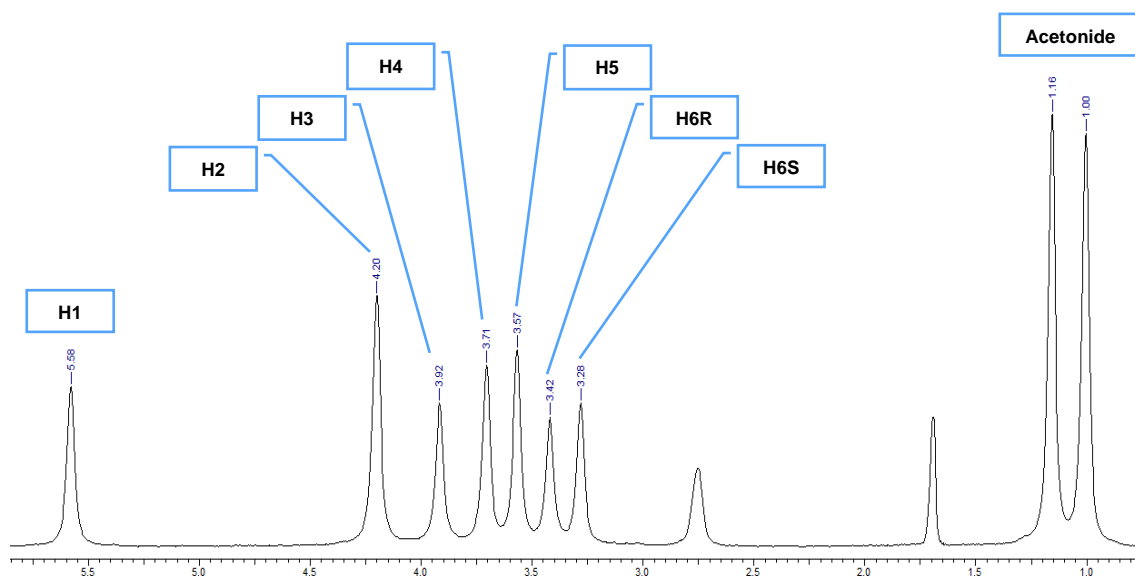


**Figure 6** Representative  $^2\text{H}$ -NMR spectrum of MAG obtained from the hepatic glycogen of a C57/BL6 mouse included in this study. The peaks corresponding to the possible deuterium enriched positions in the molecule which were used for the analysis are H5 and H6S.

Since  $^2\text{H}$ -enriched body water (BW) is the precursor for all  $^2\text{H}$ -enriched sites of glycogen glucosyl, it is necessary to measure BW in order to determine the fractional rate of  $^2\text{H}$ -incorporation into each glucosyl position which in turn allows fractional indirect pathway rates to be determined (Equations 17-19). To determine BW, deuterium

enrichment of plasma water was determined by a separate  $^2\text{H}$ -NMR assay (Figure 7, Equation 16).<sup>217</sup>

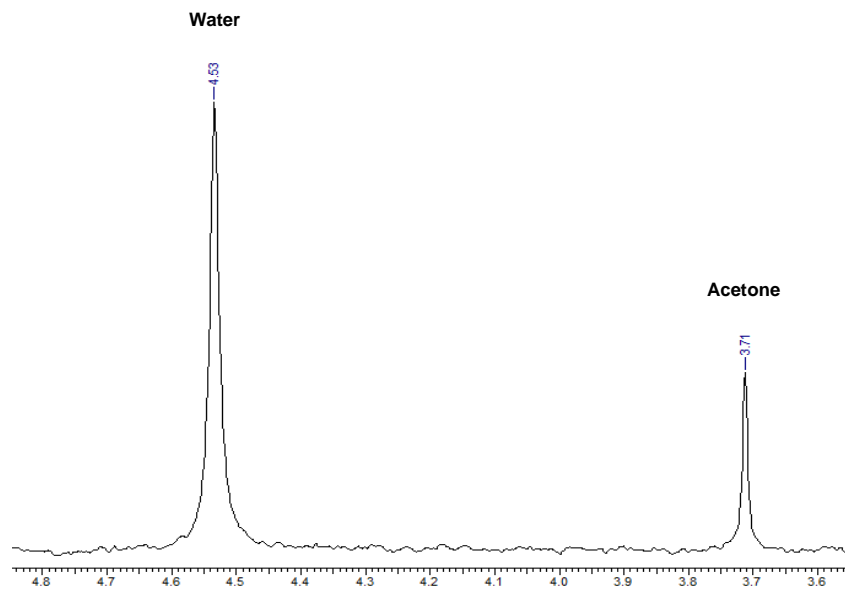


**Figure 7** Representative  $^2\text{H}$ -NMR spectrum of plasma obtained from a C57/BL6 mouse included in this study. The peak on the right corresponds to the natural-abundance  $^2\text{H}$  from the methyl hydrogen of acetone, which serves as an internal enrichment standard, and the one on the left is from the water hydrogens. The relationship between the acetone and water signals is established beforehand by performing a calibration curve with known  $^2\text{H}$ -enriched water standards and is also adjusted for the plasma protein content (assumed to be 3% of total plasma weight).

$$BW = \frac{\text{Water hydrogens}}{\text{Acetone CH}_3 \text{ hydrogens}} \times \text{calibration constant} \times 100\% \quad (16)$$

Equation 17 measures total indirect pathway contribution to glycogen synthesis derived from all sources (ID).

$$ID = \frac{{}^2\text{H}_5}{BW} \times 100\% \quad (17)$$

The Krebs cycle contribution to the indirect pathway ( $ID_{\text{KC}}$ ) was calculated with equation 18, and the contribution of triose phosphate sources to the indirect pathway ( $ID_{\text{TP}}$ ) was calculated using equation 19.

$$ID_{\text{KC}} = \frac{{}^2\text{H}_{6S}}{BW} \times 100\% \quad (18)$$

$$ID_{TP} = \frac{{}^2H_5 - {}^2H_{6S}}{BW} \times 100\% \quad (19)$$

## 2. Glycogen $^{13}C$ -enrichment derived from $[U-^{13}C_6]$ fructose

Carbon has two stable isotopes,  $^{12}C$  and  $^{13}C$ . Although  $^{12}C$  is the most naturally abundant (98.89%), it is not NMR-observable, while  $^{13}C$  (1,11% abundance) can be observed by NMR. The  $^{13}C$  signal can be split by spin-spin coupling with bound protons as well as from binding to other  $^{13}C$  nuclei. Therefore, in the absence of enrichment from  $^{13}C$ -enriched tracers, each glycogen carbon is enriched with the 1,11% background. Moreover, because of this low enrichment level, the probability of a  $^{13}C$  bound to another neighbouring  $^{13}C$  is very low. Therefore, in the presence of proton-decoupling, which abolishes  $^{13}C$  signal splitting from bound protons, the natural-abundance  $^{13}C$  signal appears as a singlet. If glycogen is enriched by  $^{13}C$  that is bound to one or more neighbouring  $^{13}C$  nuclei, the resulting  $^{13}C$  signals are split as a result of  $^{13}C$ - $^{13}C$  spin-spin coupling and are thus fully resolved from the background  $^{13}C$  singlet signal. This is the basis for using  $[U-^{13}C_6]$ fructose to trace fructose incorporation into glycogen, since glucosyl molecules synthesized from this tracer will contain connected  $^{13}C$  nuclei, referred to as isotopomers. Moreover, since the  $^{13}C$  background singlet signal represents 1,11% enrichment, it can be used as an intramolecular enrichment standard to determine the enrichments of the split isotopomer  $^{13}C$  signals.

The six hexose carbons in the MAG  $^{13}C$ -NMR spectrum are fully resolved allowing the evaluation of each carbon position of the glucose units derived from glycogen digestion. Uniformly labelled fructose metabolism gives rise to several  $^{13}C$ -isotopomers of glycogen according to the metabolic route(s) taken. In order to quantify fructose contribution to glycogen synthesis via trioses phosphate and Krebs cycle routes the fractional enrichments of  $[4,5,6-^{13}C_3]$ - and  $[5,6-^{13}C_2]$ glycogen need to be quantified (Equations 20 and 21). These were obtained by analysis of MAG position 5 (C5). This signal contains a quartet (C5Q456) representing  $[4,5,6-^{13}C_3]$ glycogen, a doublet representing  $[4,5-^{13}C_2]$ glycogen (C5D45), a doublet representing  $[5,6-^{13}C_2]$ glycogen (C5D56) and a singlet representing the 1,11% natural-abundance enrichment of carbon 5 (C5S). An illustration of this multiplet is represented on Figure 8.

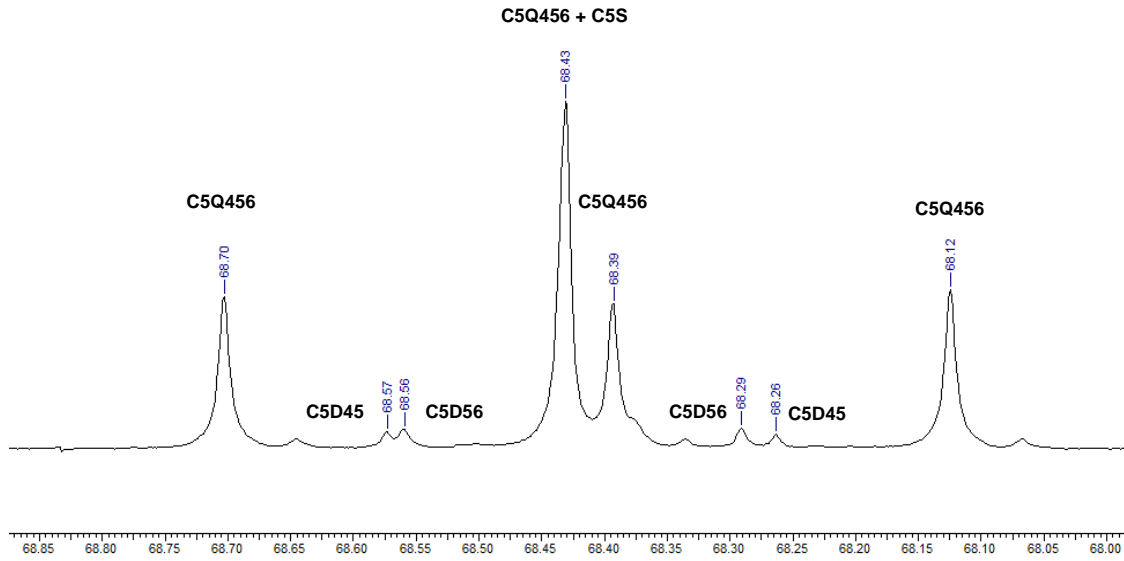


**Figure 8** Carbon 5 multiplet from a representative  $^{13}\text{C}$ -NMR spectrum of MAG obtained from the hepatic glycogen of a C57/BL6 mouse included in this study. The peaks corresponding to the quartet representing  $[4,5,6-^{13}\text{C}_3]\text{glucose}$  (C5Q456), the doublet from glucose enriched in both positions 4 and 5,  $[4,5-^{13}\text{C}_2]\text{glucose}$  (C5D45), the doublet from glucose enriched in both positions 5 and 6,  $5,6-^{13}\text{C}_2]\text{glucose}$  (C5D56), and the singlet from the 1.11% natural-abundance  $^{13}\text{C}$  (C5S) are labelled accordingly.

The enrichment of  $[5,6-^{13}\text{C}_2]\text{glycogen}$  and  $[4,5,6-^{13}\text{C}_3]\text{glycogen}$  were calculated according to equations 20 and 21, respectively. For both equations, 1,11 represents the natural abundance of  $^{13}\text{C}$ , which corresponds to the C5S signal.

$$[5,6-^{13}\text{C}_2]\text{glycogen} = \frac{\text{C5D56}}{\text{C5S}} \times 1,11 \quad (20)$$

$$[4,5,6-^{13}\text{C}_3]\text{glycogen} = \frac{\text{C5Q456}}{\text{C5S}} \times 1,11 \quad (21)$$

From equation 21, we can extrapolate the fraction of the enrichment in  $[4,5,6-^{13}\text{C}_3]\text{glycogen}$  derived from the trioses phosphate as enunciated on equation 22.

$$[4,5,6-^{13}\text{C}_3]\text{glycogen}_{TP} = [4,5,6-^{13}\text{C}_3]\text{glycogen} - [4,5,6-^{13}\text{C}_3]\text{glycogen}_{KC} \quad (22)$$

Enrichment of [4,5,6-<sup>13</sup>C<sub>3</sub>]glycogen, derived via the Krebs cycle ([4,5,6-<sup>13</sup>C<sub>3</sub>]glycogen) is related to that of [5,6-<sup>13</sup>C<sub>2</sub>]glycogen, by a constant (0,67) and was therefore calculated accordingly by equation 23.<sup>221</sup>

$$[4,5,6 - ^{13}\text{C}_3]\text{-glycogen}_{KC} = [5,6 - ^{13}\text{C}_2]\text{glycogen} \times 0,67 \quad (23)$$

The contribution of exogenous fructose to total glycogen synthesis via the Krebs cycle (Fructose<sub>KC</sub>) and triose phosphates (Fructose<sub>TP</sub>) were calculated from equations 24 and 25. For equation 24, the 1,67 and 1,5 constants account for isotope scrambling and dilution at the level of the Krebs cycle, respectively.<sup>219</sup> The 100/20 constant in both equations accounts for the fact that the exogenous fructose was 20% enriched.

$$Fructose_{KC} = \frac{[5,6 - ^{13}\text{C}_2]\text{-glycogen}_{KC}}{100} \times 1,67 \times 1,5 \times \frac{100}{20} \% \quad (24)$$

$$Fructose_{TP} = \frac{[4,5,6 - ^{13}\text{C}_3]\text{-glycogen}_{TP}}{100} \times \frac{100}{20} \% \quad (25)$$

Finally, the contribution of exogenous fructose to each of the indirect pathway components (Ind TP and Ind KC) was calculated from equations 26 and 27.

$$Ind\ TP\ from\ Fructose = \frac{Fructose_{TP}}{ID_{TP}} \times 100\% \quad (26)$$

$$Ind\ KC\ from\ Fructose = \frac{Fructose_{KC}}{ID_{KC}} \times 100\% \quad (27)$$

## Statistical analysis

Data organization, flux calculations and some preliminary corrections were performed in Microsoft Excel (Office 365, 2002) and the statistical analysis was conducted in GraphPad Prism 7.00 (GraphPad Inc.).

Before performing statistical tests, all groups were tested for normality (Shapiro-Wilk test) and homoscedasticity (Bartlett's test for One-way ANOVA and F test for Student's T test). If both normality and homoscedasticity were confirmed, parametric tests were applied. In case normality failed, the equivalent non-parametric test was used, and for groups where homoscedasticity failed, the appropriate corrections were employed. In addition, all the experimental conditions were subjected to the ROUT method to identify outliers, but no outlier was found.

In particular, for the analysis of two groups with normal distribution, a Student's T test was applied, with a Welch correction if the dataset lacked homoscedasticity. In opposition, when the dataset failed the normality test, the Mann-Whitney test was applied. In both cases, the results were represented in the form of bars with means and standard deviations.

When comparing more than 2 groups, a One-way ANOVA was used with a Tukey post-test for multiple comparisons, unless the dataset failed the normality test. In that case, the non-parametric equivalent, which is the Kruskal-Wallis test with Dunn's post-test for multiple comparisons, was applied. For One-way ANOVA with Tukey post-test, data was expressed in graphs of box plots with means (+) plus Tukey whiskers, while for Kruskal-Wallis, graphs were represented as box plots with means (+) plus min to max whiskers.

All statistical analysis was done considering a 95% confidence interval, which means that the groups were only considered significantly different when p-value was below 0,05 ( $p < 0,05$ ).



# Results

---

## 1. Hepatic Glycogen quantification

Figure 9 shows the results obtained from hepatic glycogen quantification according to the protocol described by Keppler and Decker.<sup>222</sup> Hepatic glycogen concentration did not significantly vary according to diet composition. The HF mice had the smallest amount of glycogen in their livers ( $370,656 \pm 113,217$  mmol/g of tissue), followed by HS ( $467,262 \pm 205,125$  mmol/g of tissue), HFHS ( $487,100 \pm 142,410$  mmol/g of tissue) and, finally, SC ( $498,888 \pm 148,942$  mmol/g of tissue). In this way, diet composition did not affect glycogen concentration in the liver.

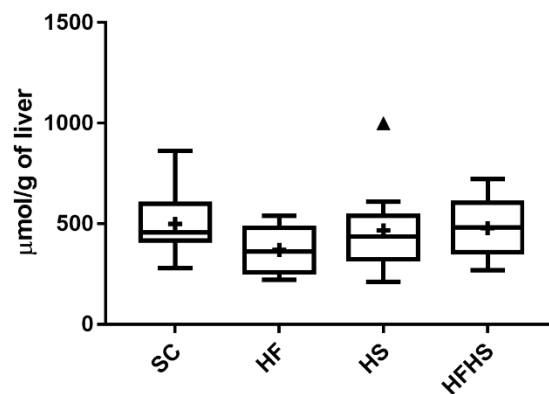


**Figure 9** Graph depicting the concentration of hepatic glycogen at the moment of the euthanization. Statistical analysis was performed using One-way ANOVA of multiple comparisons according to the Tukey's post-test. No statistically significant differences were identified. The + sign indicates the mean of each group and the triangle indicates the maximum of the HS group, which is not an outlier. The amount of glycogen in SC mice was  $499 \pm 149$  µmol/g of liver, in HF mice is  $371 \pm 113$  µmol/g of liver, in HS mice is  $467 \pm 205$  µmol/g of liver and in HFHS mice is  $487 \pm 142$  µmol/g of liver.

## 2. Sources of hepatic glycogen synthesis

Figure 10 shows the results obtained from the analysis of the indirect pathway contribution to glycogenesis. It shows that diet composition had an impact on the direct to indirect pathway ratio, even though it did not affect the net amount of glycogen in the liver. Furthermore, the indirect pathway was only the main contributor to glycogen synthesis in the HF diet.

The SC group demonstrated the smallest indirect pathway (32,49 ± 7,526 %) contribution to total glycogen levels, suggesting that these animals either synthesized most of their hepatic glycogen via the direct pathway and/or had significant amounts of pre-existing glycogen. The highest indirect pathway contribution was registered by mice under HF feeding which was statistically different from SC (58 ± 8 % vs 32 ± 8 % p<0,05), suggesting that fat intake increased indirect pathway activity to a point at which it became the main contributor to glycogen synthesis.

The HS diet had significantly lower indirect pathway contributions to total glycogen levels compared to the HF group (37 ± 9% vs 58 ± 8%, p<0,05), achieving a comparable contribution to SC animals. The animals fed the HFHS diet also had significantly lower indirect pathway contributions compared to HF mice (40 ± 4 % vs 58 ± 8%, p<0,05), but were not significantly different from HS. These observations are consistent with fructose promoting the flux through the direct pathway, counteracting the decrease associated with fat intake.

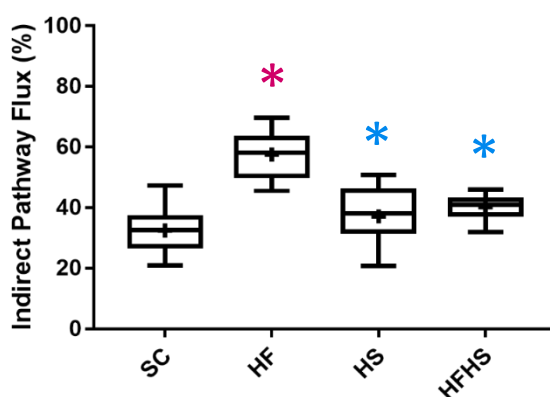


**Figure 10** Graph depicting the results of the evaluation the Indirect Pathway contribution to glycogen synthesis using <sup>2</sup>H-enrichment NMR analysis of liver MAG. The statistical analysis performed in this case was One-way ANOVA of multiple comparisons with Tuckey's post-test, which indicates that the HF group is significantly different from the SC group (\*p<0,05), while the HS and HFHS mice are statistically different from the HF group (\*p<0,05).

In this study we were also interested in assessing which were the main substrate precursors fuelling the indirect pathway, in particular those derived from trioses phosphate and the Krebs cycle.

Figure 11 shows the results from the Krebs cycle contribution to the indirect pathway. Our data shows that HF feeding favoured the use of the Krebs cycle

intermediates as substrates for hepatic glycogen synthesis (HF:  $44 \pm 7\%$  vs SC:  $21 \pm 6\%$ ).

The HS group showed the smallest contribution derived from the Krebs cycle, which was significantly different from that registered for the HF group ( $14 \pm 7\%$  vs  $44 \pm 7\%$ ,  $p < 0,05$ ), but comparable to the SC condition. The HFHS group demonstrated a slightly higher contribution to the indirect pathway derived from Krebs cycle, which was not significantly different from the HS or SC group, but was significantly different from the HF group ( $21 \pm 6\%$  vs  $44 \pm 7\%$ ,  $p < 0,05$ ).

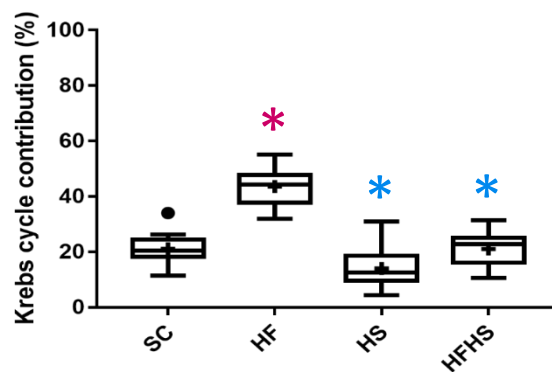


**Figure 11** Graph depicting the results obtained from  $^2\text{H}$ -enrichment NMR analysis of position 6S of liver MAG. The statistical analysis performed in this case was One-way ANOVA of multiple comparisons with Tuckey's post-test, which indicates that the HF group is significantly different from the SC group ( $*p < 0,05$ ), while the HS and HFHS conditions are statistically different from the HF condition ( $*p < 0,05$ ).

Figure 12 depicts the trioses phosphate contribution to the indirect pathway of glycogen synthesis. The groups resorting the most to the trioses phosphate were those supplemented with HFCS-55, especially the ones on the HS diet. This group's use of the trioses phosphate for glycogen synthesis was significantly higher compared to SC ( $23 \pm 6\%$  vs  $11 \pm 3\%$ ,  $p < 0,05$ ) and the HF groups ( $23 \pm 6\%$  vs  $14 \pm 1\%$ ,  $p < 0,05$ ). These suggest that, although fructose might be stimulating glucose utilization via the direct pathway, it is nevertheless contributing to gluconeogenesis at the level of trioses phosphate.

HFHS mice use of trioses phosphate for glycogen synthesis was increased compared to the SC condition ( $19 \pm 3\%$  vs  $11 \pm 3\%$ ,  $p < 0,05$ ), but similar to both HF ( $19 \pm 3\%$  vs  $14 \pm 1\%$ ) and HS groups ( $19 \pm 3\%$  vs  $23 \pm 6\%$ ).

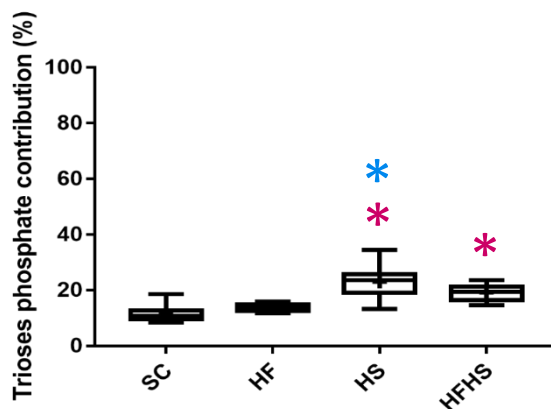


**Figure 12** Graph depicting the results of the  $^2\text{H}$ -enrichment NMR analysis of position 5 of liver MAG. The statistical analysis performed in this case was Kruskal-Wallis test of multiple comparison with Dunn's post-test, which indicates that the HS and HFHS conditions are statistically different from the SC group (\* $p < 0,05$ ) and the HS is also different from the HF group (\* $p < 0,05$ ).

Figure 13 demonstrates the direct comparison between the contributions of the trioses phosphate and the Krebs cycle to the indirect pathway obtained for each group. It is noticeable that mice who were not supplemented with HFCS-55 (SC and HF) showed an increased preference for the Krebs cycle precursors. High-fat feeding caused a substantial increase in this preference, which may be due to the elevated amount of Acetyl-CoA stimulating pyruvate carboxylase.

In contrast, the preferred source of precursors in the HS group was triose phosphate. However, when a fat-rich diet was used together with HFCS-55 supplementation (HFHS), triose phosphate sources tended to give way to Krebs cycle precursors.

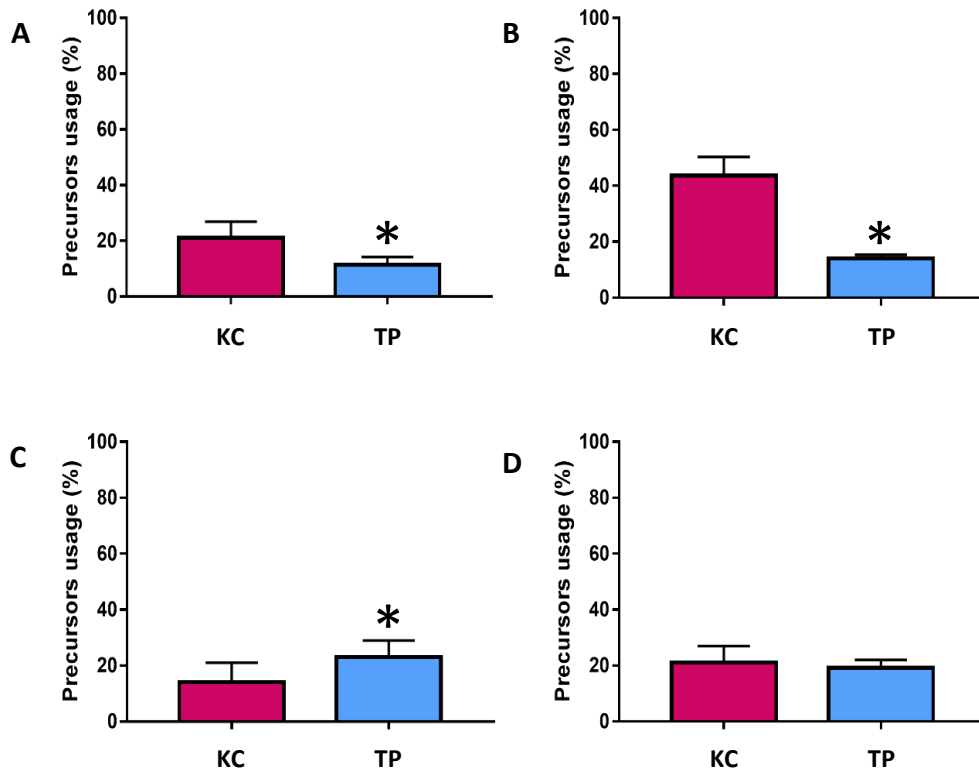
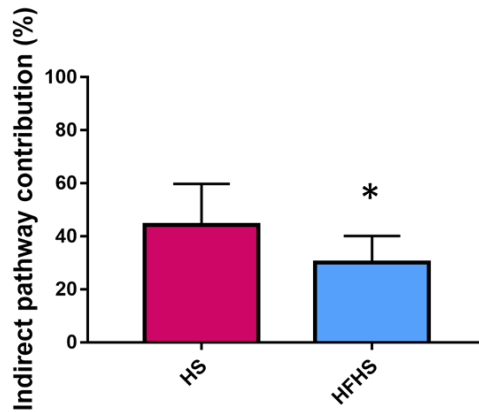


**Figure 13** Panel of graphs summarizing Krebs cycle (KC) and the Triose phosphate (TP) contributions to the indirect pathway of glycogen synthesis. Graph A represents the results from the SC group, Graph B depicts the results obtained from the HF group, Graph C shows the results obtained from the HS condition, and Graph D depicts the results from the HFHS group. The statistical analysis performed for Graph A consisted on a Mann-Whitney test, for Graph B and D consisted on an Unpaired T tests using the Welch correction and for Graph C was a standard unpaired T test.

### 3. Carbon-13 Isotopomers NMR analysis

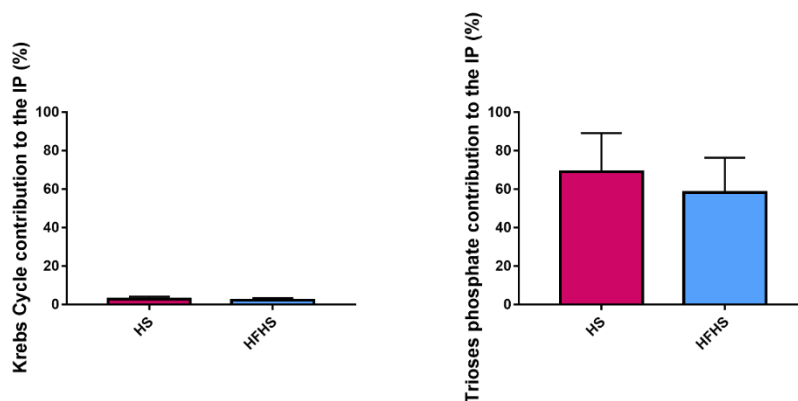
As mentioned in the objectives we were interested in assessing which pathway(s) of hepatic glycogen synthesis were fed by fructose in the setting of diet-induced NAFLD.

Figure 14 depicts the results obtained from the analysis of fructose contribution to the indirect pathway of glycogen synthesis. Our results demonstrate that fructose was incorporated into glycogen through the indirect pathway in both HS and HFHS mice. The fructose contribution to the indirect pathway in HS was significantly higher compared to HFHS ( $44 \pm 16\%$  vs  $30 \pm 10\%$ ,  $p < 0,05$ ). Possibly, fat intake led to more fructose being converted into glucose instead of glycogen via gluconeogenesis.



**Figure 14** Graph depicting the fructose contribution to the indirect pathway of glycogen synthesis in HS and HFHS mice. The statistical analysis performed in this case was a Student's T test, reaching statistical significance (\* $p < 0,05$ ).

Figure 15 shows the resolved contributions of fructose to indirect pathway fluxes via the Krebs cycle and indirect pathway fluxes via triose phosphate. Since fructose enters the gluconeogenic pathway at the level of triose phosphate, it is not surprising that it dominated the contribution of these indirect pathway sources to glycogen synthesis for the HS mice. In contrast, its contribution to indirect pathway flux via Krebs cycle was very small, indicating that only a minor portion of triose phosphates derived from fructose were converted to pyruvate and recycled via pyruvate carboxylase and PEPCK. This utilization pattern was similar for HFHS mice although there was a tendency towards a reduced contribution to indirect pathway flux from triose phosphate.



**Figure 15** Graph describing the contributions of fructose to indirect pathway flux via the Krebs Cycle (left) and via triose phosphate (right) The statistical analysis performed on the left was a Mann-Whitney test, and on the right was a Student's T test.

## Discussion

---

**The effects of the diets on postprandial hepatic glycogen levels:** Glycogen pathway contributions vary according to the nutritional state of the individual. In diets consisting of multiple meals per day separated by less than 5 hours with moderate carbohydrate content, most glycogen synthesis occurs by the direct pathway. The rate of glycogenesis decreases, while the rate of glycogenolysis increases towards the evening.<sup>225</sup> In our study, mice were euthanized in the morning after a night at which they had free access to food and were not stimulated to exercise. As a consequence, they are not fasted nor are at a stage of intense energy expenditure. Literature shows that glycogen stores are heavily influenced by fasting and exercise, since enzyme expression and activity of glycogenesis and glycogenolysis deeply vary in response to those stimuli, leading to oscillations in hepatic glycogen concentration.<sup>135,226</sup> Diet composition has also been demonstrated to influence glycogen metabolism and thus hepatic glycogen content.<sup>120,121,130</sup>

Fructose is more efficiently extracted by the liver than glucose and liver fructokinase has higher enzymatic activity and is less regulated than glucokinase.<sup>103,109,110</sup> As a consequence, fructose 1-phosphate accumulates more rapidly than glucose 6-phosphate in the fed state.<sup>105</sup> However, fructose increases glucose uptake in the liver, therefore promoting glucose 6-phosphate synthesis.<sup>227</sup> Moreover, fructose 1-phosphate allosterically inhibits glycogen phosphorylase a activity, causing glycogen synthase activation. Altogether, fructose intake should potentiate glycogen accumulation in the liver, hence we should observe increased glycogen concentration in the livers of HS mice.<sup>120,121,228</sup>

HF diets promote  $\beta$ -oxidation, leading to increased amounts of acetyl-CoA in the liver as well as increased circulating free fatty acids. Plasma free fatty acids are extracted by the liver to be assembled in triglycerides.<sup>229,230</sup> Evidence shows that increased circulation of free fatty acids leads to their deposition in the liver in the form of TG, but also DAG. As DAG accumulates in the liver, hepatic steatosis and insulin resistance develop.<sup>72-76</sup> Hepatic insulin resistance decreases glucokinase activity and promotes glycogen cycling.<sup>94</sup> Based on this, the net amount of glycogen in the liver would be expected to be reduced in this setting. High-fat high-fructose diets have been shown to increase hepatic glycogen content compared to high-fat diets alone.<sup>127</sup> Therefore, we expected to see increased hepatic glycogen concentrations in all groups compared to controls, with the HFHS group achieving the highest concentration among all.

However, our results indicate similar levels of hepatic glycogen for the four dietary conditions that were studied (Figure 9). This might be due to excessive calorie intake leading to the exhaustion of liver capacity to store glycogen and/or high amounts of pre-existing glycogen (i.e. present at the end of the light cycle). Glycogen is a highly hygroscopic molecule and excessive accumulation may impinge on normal hepatocyte function. It is possible that hepatic glycogen stores had reached their maximal levels for all experimental groups.

**The effects of the diets on the sources of hepatic glycogen synthesis:** The HF diet promotes  $\beta$ -oxidation leading to high levels of acetyl-CoA. Acetyl-CoA stimulates the activity of pyruvate dehydrogenase (PDH) kinase leading to the inhibition of the PDH complex and preventing pyruvate oxidation. In this way, pyruvate utilization by the indirect pathway via pyruvate carboxylase and the Krebs cycle is facilitated. Thus, the HF diet should favour the indirect pathway contribution to glycogen synthesis, which was consistent with our findings (see Figure 10).<sup>229,230</sup>

The HS diet consists of normal chow supplemented with both fructose and glucose in drinking water to mimic HFCS-55. As mentioned before, fructose is not only more efficiently extracted by the liver and metabolized by fructokinase, but its fructose 1-phosphate product also stimulates glucokinase and increases glucose uptake. Moreover, fructose 1-phosphate allosterically inhibits glycogen phosphorylase activity, causing glycogen synthase activation. Thus, fructose participates in the indirect pathway as a substrate, while at the same time stimulating glucose usage by the direct pathway.<sup>103,105,109,110,120,121,227,228,231</sup> In fact, our results show that the HS diet had a comparable indirect/direct pathway profile to that of SC, but a significant decrease of indirect pathway contribution compared to the HF diet (Figure 10). Thus, we conclude that fructose maintains glucose conversion to glycogen through the mechanisms described.

Even though current knowledge suggests that high-fat high-fructose diets might impact direct pathway activity via hepatic insulin resistance, our data demonstrates a preservation of direct pathway activity in this setting. Fat intake promotes insulin resistance, decreases glucokinase activity and stimulates glycogen cycling.<sup>94</sup> By supplementing the HF chow with HFCS-55, we increased the availability of both fructose and glucose. Fructose will prevent glucokinase inhibition and increase glucose uptake, improving glucose tolerance.<sup>130,228,231</sup> In this way, fructose opposes the negative effects of fats in glucose uptake and glycogenesis thereby counteracting the dominance of indirect pathway activity exerted by the HF diet (Figure 10).<sup>130</sup> As previously mentioned,



HF diets promote the accumulation of acetyl-CoA which not only inhibits the PDH complex, but also stimulates the activity of pyruvate carboxylase. As a result, pyruvate is converted to oxaloacetate to replenish Krebs cycle intermediates, instead of being oxidized to acetyl-CoA.<sup>51,229,230</sup> Oxaloacetate can be then used for gluconeogenesis or glycogen synthesis via the indirect pathway. This concurs with our observations of the majority of indirect pathway carbons being derived via the Krebs cycle in HF mice (Figure 11, 12 and 13). Fructose enters both glycolysis and gluconeogenesis at the level of triose phosphate, therefore the main source of gluconeogenic precursors in the HS group are expected to be derived from this pathway with very little contribution from the Krebs cycle.<sup>103,109,110</sup> Our data were concordant with this premise (Figure 11, 12 and 13).

HFHS mice showed similar glycogen synthesis profiles to the HS group (Figure 11 and 12), suggesting that HFCS supplementation was counteracting against the reduced direct pathway. Since fructose promotes *de novo* lipogenesis, acetyl-CoA generation from  $\beta$ -oxidation might be inhibited by malonate. This would in turn prevent inhibition of PDH and pyruvate would be oxidized instead of being carboxylated for gluconeogenesis.<sup>94,130,228,231</sup> This is concordant with our observation that HFHS mice were the only ones not showing a preference between the Krebs cycle precursors and the triose phosphate (Figure 13). Finally, SC chow mice showed a preference for glycogen synthesis via the Krebs cycle intermediates to perform glycogen synthesis, indicating that the indirect pathway activity is a normal component of hepatic glycogen synthesis.

**The effects of high fat feeding on the metabolism of HFCS-fructose:** Fructose enters the indirect pathway via triose phosphate leading to its incorporation into glycogen (Figures 14 and 15). We believe this is the first time that fructose incorporation into glycogen was demonstrated in an early-stage NAFLD model. There were no differences between the rate of incorporation into glycogen of trioses phosphate or Krebs cycle intermediates derived from fructose (Figure 15), but there was a statistically significant difference between HS and HFHS mice in the indirect pathway contributions derived from fructose (Figure 14). These suggest that some of the fructose might be converted to glucose, instead of glycogen. HFHS mice are possibly channelling some substrates for glucose production to be directly exported to the blood, while HS mice are channelling substrates for glucose storage via the indirect pathway of glycogen synthesis.

Nevertheless, HFCS-55 not only fuels the indirect pathway of glycogen synthesis with fructose, but also improves glucose tolerance by stimulating glucose uptake by the liver and increased upregulation of the direct pathway of glycogen synthesis via glucokinase stimulation (Figures 11, 12 and 13). In this way, even though high-fat high-sugar diets are more efficient in promoting the development of NAFLD, it also seems that HFCS-55 counteracts some of the metabolic effects of high-fat feeding regarding glycogen synthesis (Figure 10). In the future, it would be interesting to evaluate the amount of food ingested by each group to see if diet composition, especially HFCS-55 supplementation can affect food intake as suggested by Lopez-Soldado et al.<sup>183</sup>

## Conclusion

---

The incidence of NAFLD in the world is high and will continue to grow, representing an increasing burden to health care systems worldwide. NAFLD was long considered the hepatic manifestation of the metabolic syndrome, but the increasing number of cases among lean subjects who lack other features of this syndrome, are a growing concern.<sup>3,232</sup> Moreover, the world is currently facing the coronavirus disease 2019 (COVID-19) pandemic, which long-term effects include liver damage at least for one-third of the infected, therefore it is highly probable that more people than estimated are now predisposed to liver disease. Furthermore, NAFLD might have a role in the outcome of COVID-19 patients. In this way, it has never been more important to establish proper diagnosis and therapies.<sup>233,234</sup>

Excessive intake of fat and refined sugars, especially fructose, is known to be an important risk factor for NAFLD.<sup>191,192,209–215</sup> Therefore, the food industry must be stressed by governments to reduce added sugars, especially HFCS. In many Western countries, there is now a so-called “sugar tax” that is levied on the sugar content of food and drink products. In Portugal, according to law number 30/2019, the advertisement of highly energetic food products with high concentrations of salt, refined sugars, saturated fatty acids and/or transformed fatty acids directed to subjects under 16 years old is restricted since 23<sup>rd</sup> of April 2019.<sup>235</sup>

In this study, we have shown that hepatic glycogen concentration is not necessarily affected by diet composition in the context of NAFLD. High-fat feeding increases the indirect pathway contribution to glycogen synthesis, possibly by promoting the accumulation of acetyl-CoA, which in turn stimulates pyruvate carboxylation and consequently gluconeogenesis. Since fructose can improve hepatic glucose metabolism by increasing glucose uptake and the activity of glucokinase, HFCS-55 supplementation increases the direct pathway contribution to glycogen synthesis. Moreover, in mice under high-fat feeding, HFCS-55 prevents the increase in the indirect pathway contribution observed in mice fed high-fat diet only. In this way, even though high-fat high-sugar diets are more efficient in promoting the development of NAFLD, it also appears that HFCS-55 counteracts the effects of high-fat feeding on the sources of hepatic glycogen synthesis.

Finally, we demonstrated directly the incorporation of exogenous fructose into hepatic glycogen via the indirect pathway of glycogen synthesis while at the same time stimulating glucose usage by the direct pathway in an obesogenic setting.

One of the shortcomings this study was the absence of basal hepatic glycogen data (which would have required duplicating the number of mice for the study). Thus, we cannot be sure that the glycogen quantified was entirely produced during the night from which our fluxes were calculated (pre-existing). Finally, we also should monitor food intake, to determine the extent to which diet composition influences hunger and satiety.

## References

---

1. Paul, S. & Davis, A. M. Diagnosis and Management of Nonalcoholic Fatty Liver Disease. *JAMA* **320**, 2474 (2018).
2. Younossi, Z. M. *et al.* Global epidemiology of nonalcoholic fatty liver disease—Meta-analytic assessment of prevalence, incidence, and outcomes. *Hepatology* **64**, 73–84 (2016).
3. Younossi, Z. *et al.* Global Perspectives on Nonalcoholic Fatty Liver Disease and Nonalcoholic Steatohepatitis. *Hepatology* **69**, 2672–2682 (2019).
4. EASL–EASD–EASO Clinical Practice Guidelines for the management of non-alcoholic fatty liver disease. *J. Hepatol.* **64**, 1388–1402 (2016).
5. Estes, C. *et al.* Modeling NAFLD disease burden in China, France, Germany, Italy, Japan, Spain, United Kingdom, and United States for the period 2016–2030. *J. Hepatol.* **69**, 896–904 (2018).
6. Cohen, J. C., Horton, J. D. & Hobbs, H. H. Human fatty liver disease: old questions and new insights. *Science* **332**, 1519–23 (2011).
7. Lindenmeyer, C. C. & McCullough, A. J. The Natural History of Nonalcoholic Fatty Liver Disease—An Evolving View. *Clin. Liver Dis.* **22**, 11–21 (2018).
8. Younossi, Z. M., Marchesini, G., Pinto-Cortez, H. & Petta, S. Epidemiology of Nonalcoholic Fatty Liver Disease and Nonalcoholic Steatohepatitis: Implications for Liver Transplantation. *Transplantation* **103**, 22–27 (2019).
9. Chen, F. *et al.* Lean NAFLD: A Distinct Entity Shaped by Differential Metabolic Adaptation. *Hepatology* hep.30908 (2019). doi:10.1002/hep.30908
10. Kawaguchi-Suzuki, M. *et al.* A Genetic Score Associates With Pioglitazone Response in Patients With Non-alcoholic Steatohepatitis. *Front. Pharmacol.* **9**, 752 (2018).
11. Chalasani, N. *et al.* The diagnosis and management of nonalcoholic fatty liver disease: Practice guidance from the American Association for the Study of Liver Diseases. *Hepatology* **67**, 328–357 (2018).
12. Chalasani, N. *et al.* The diagnosis and management of non-alcoholic fatty liver disease: Practice Guideline by the American Association for the Study of Liver Diseases, American College of Gastroenterology, and the American Gastroenterological Association. *Hepatology* **55**, 2005–2023 (2012).
13. McPherson, S. *et al.* Magnetic resonance imaging and spectroscopy accurately estimate the severity of steatosis provided the stage of fibrosis is considered. *J. Hepatol.* **51**, 389–397 (2009).
14. Angulo, P. *et al.* The NAFLD fibrosis score: A noninvasive system that identifies liver fibrosis in patients with NAFLD. *Hepatology* **45**, 846–854 (2007).
15. Vallet-Pichard, A. *et al.* FIB-4: An inexpensive and accurate marker of fibrosis in HCV infection. Comparison with liver biopsy and FibroTest. *Hepatology* **46**, 32–36 (2007).
16. Patton, H. *et al.* Clinical correlates of histopathology in pediatric nonalcoholic steatohepatitis (NASH). *Gastroenterology* **135**, 1961 (2008).

17. Kleiner, D. E. *et al.* Design and validation of a histological scoring system for nonalcoholic fatty liver disease. *Hepatology* **41**, 1313–1321 (2005).
18. Bedossa, P. *et al.* Histopathological algorithm and scoring system for evaluation of liver lesions in morbidly obese patients. *Hepatology* **56**, 1751–1759 (2012).
19. Angulo, P. *et al.* Liver fibrosis, but no other histologic features, is associated with long-term outcomes of patients with nonalcoholic fatty liver disease. *Gastroenterology* **149**, 389-397.e10 (2015).
20. Dulai, P. S. *et al.* Increased risk of mortality by fibrosis stage in nonalcoholic fatty liver disease: Systematic review and meta-analysis. *Hepatology* **65**, 1557–1565 (2017).
21. Musso, G., Cassader, M., Rosina, F. & Gambino, R. Impact of current treatments on liver disease, glucose metabolism and cardiovascular risk in non-alcoholic fatty liver disease (NAFLD): A systematic review and meta-analysis of randomised trials. *Diabetologia* **55**, 885–904 (2012).
22. Wu, T., Gao, X., Chen, M. & Van Dam, R. M. Long-term effectiveness of diet-plus-exercise interventions vs. diet-only interventions for weight loss: A meta-analysis: Obesity Management. *Obes. Rev.* **10**, 313–323 (2009).
23. Vilar-Gomez, E. *et al.* Weight loss through lifestyle modification significantly reduces features of nonalcoholic steatohepatitis. *Gastroenterology* **149**, 367-378.e5 (2015).
24. Haufe, S. *et al.* Randomized comparison of reduced fat and reduced carbohydrate hypocaloric diets on intrahepatic fat in overweight and obese human subjects. *Hepatology* **53**, 1504–1514 (2011).
25. Kirk, E. *et al.* Dietary Fat and Carbohydrates Differentially Alter Insulin Sensitivity During Caloric Restriction. *Gastroenterology* **136**, 1552–1560 (2009).
26. St. George, A. *et al.* Independent effects of physical activity in patients with nonalcoholic fatty liver disease. *Hepatology* **50**, 68–76 (2009).
27. Kistler, K. D. *et al.* Physical activity recommendations, exercise intensity, and histological severity of nonalcoholic fatty liver disease. *Am. J. Gastroenterol.* **106**, 460–468 (2011).
28. Sung, K. C. *et al.* Effect of exercise on the development of new fatty liver and the resolution of existing fatty liver. *J. Hepatol.* **65**, 791–797 (2016).
29. Erhardt, A. *et al.* Plasma levels of vitamin E and carotenoids are decreased in patients with nonalcoholic steatohepatitis (NASH). *Eur. J. Med. Res.* **16**, 76–78 (2011).
30. Xu, R., Tao, A., Zhang, S., Deng, Y. & Chen, G. Association between vitamin E and non-alcoholic steatohepatitis: A meta-analysis. *Int. J. Clin. Exp. Med.* **8**, 3924–3934 (2015).
31. Sato, K. *et al.* Vitamin E has a beneficial effect on nonalcoholic fatty liver disease: A meta-analysis of randomized controlled trials. *Nutrition* **31**, 923–930 (2015).
32. Sanyal, A. J., Abdelmalek, M. F., Suzuki, A., Cummings, O. W. & Chojkier, M. No significant effects of ethyl-eicosapentanoic acid on histologic features of nonalcoholic steatohepatitis in a phase 2 trial. *Gastroenterology* **147**, 377–84.e1 (2014).
33. Lindor, K. D. *et al.* Ursodeoxycholic Acid for Treatment of Nonalcoholic

- Steatohepatitis: Results of a Randomized Trial. *Hepatology* **39**, 770–778 (2004).
34. Dufour, J. F. *et al.* Randomized Placebo-Controlled Trial of Ursodeoxycholic Acid With Vitamin E in Nonalcoholic Steatohepatitis. *Clin. Gastroenterol. Hepatol.* **4**, 1537–1543 (2006).
  35. Lassailly, G. *et al.* Bariatric surgery reduces features of nonalcoholic steatohepatitis in morbidly obese patients. *Gastroenterology* **149**, 379–388 (2015).
  36. Mathurin, P. *et al.* Prospective Study of the Long-Term Effects of Bariatric Surgery on Liver Injury in Patients Without Advanced Disease. *Gastroenterology* **137**, 532–540 (2009).
  37. Yuan, L. & Terrault, N. A. PNPLA3 and nonalcoholic fatty liver disease: towards personalized medicine for fatty liver. *Hepatobiliary Surg. Nutr.* **9**, 353–356 (2020).
  38. Unger, R. H., Dobbs, R. E. & Orci, L. Insulin, Glucagon, and Somatostatin Secretion in the Regulation of Metabolism. *Annu. Rev. Physiol.* **40**, 307–343 (1978).
  39. BALKS, H.-J. & JUNGERMANN, K. Regulation of peripheral insulin/glucagon levels by rat liver. *Eur. J. Biochem.* **141**, 645–650 (1984).
  40. Nakamura, A. & Terauchi, Y. Lessons from Mouse Models of High-Fat Diet-Induced NAFLD. *Int. J. Mol. Sci.* **14**, 21240–21257 (2013).
  41. Witters, L. A. & Avruch, J. Insulin Regulation of Hepatic Glycogen Synthase and Phosphorylase. *Biochemistry* **17**, 406–410 (1978).
  42. Kruszynska, Y. T., Home, P. D. & Alberti, K. G. M. M. In vivo regulation of liver and skeletal muscle glycogen synthase activity by glucose and insulin. *Diabetes* **35**, 662–667 (1986).
  43. Lee, J. & Kim, M. S. The role of GSK3 in glucose homeostasis and the development of insulin resistance. *Diabetes Res. Clin. Pract.* **77**, S49–S57 (2007).
  44. McManus, E. J. *et al.* Role that phosphorylation of GSK3 plays in insulin and Wnt signalling defined by knockin analysis. *EMBO J.* **24**, 1571–1583 (2005).
  45. Brubaker, P. L. & Drucker, D. J. Structure-Function of the Glucagon Receptor Family of G Protein-Coupled Receptors: The Glucagon, GIP, GLP-1, and GLP-2 Receptors. *Recept. Channels* **8**, 179–188 (2002).
  46. Li, X. C., Carretero, O. A., Shao, Y. & Zhuo, J. L. Glucagon receptor-mediated extracellular signal-regulated kinase 1/2 phosphorylation in rat mesangial cells: Role of protein kinase A and phospholipase C. in *Hypertension* **47**, 580–585 (Hypertension, 2006).
  47. Cho, Y. M., Merchant, C. E. & Kieffer, T. J. Targeting the glucagon receptor family for diabetes and obesity therapy. *Pharmacology and Therapeutics* **135**, 247–278 (2012).
  48. Xu, Y. & Xie, X. Glucagon receptor mediates calcium signaling by coupling to Gαq/11 and Gαi/o in HEK293 cells. *J. Recept. Signal Transduct.* **29**, 318–325 (2009).
  49. Claus, T. H., Schlumpf, J. R., El-Maghrabi, M. R., Pilkis, J. & Pilkis, S. J. Mechanism of action of glucagon on hepatocyte phosphofructokinase activity. *Proc. Natl. Acad. Sci. U. S. A.* **77**, 6501–6505 (1980).

50. van den Berg, G. B., van Berkel, T. J. C. & Koster, J. F. Cyclic AMP-dependent inactivation of human liver pyruvate kinase. *Biochem. Biophys. Res. Commun.* **82**, 859–864 (1978).
51. Nelson, D. L. . C. M. M. *Lehninger Principles of Biochemistry*. (W. H. Freeman and Company, 2013).
52. Drucker, D. J. Glucagon-like peptides. *Diabetes* **47**, 159–169 (1998).
53. Bernsmeier, C. *et al.* Glucose-Induced Glucagon-Like Peptide 1 Secretion Is Deficient in Patients with Non-Alcoholic Fatty Liver Disease. *PLoS One* **9**, e87488 (2014).
54. Gupta, N. A. *et al.* Glucagon-like peptide-1 receptor is present on human hepatocytes and has a direct role in decreasing hepatic steatosis in vitro by modulating elements of the insulin signaling pathway. *Hepatology* **51**, 1584–1592 (2010).
55. Ben-Shlomo, S. *et al.* Glucagon-like peptide-1 reduces hepatic lipogenesis via activation of AMP-activated protein kinase. *J. Hepatol.* **54**, 1214–1223 (2011).
56. Baldassano, S., Amato, A., Rappa, F., Cappello, F. & Mulè, F. Influence of endogenous glucagon-like peptide-2 on lipid disorders in mice fed a high-fat diet. *Endocr. Res.* **41**, 317–324 (2016).
57. Moore, B. A. *et al.* GLP-2 receptor agonism ameliorates inflammation and gastrointestinal stasis in murine postoperative ileus. *J. Pharmacol. Exp. Ther.* **333**, 574–583 (2010).
58. Okubo, H. *et al.* Roles of gut-derived secretory factors in the pathogenesis of non-alcoholic fatty liver disease and their possible clinical applications. *International Journal of Molecular Sciences* **19**, (2018).
59. Yong, H. L. & White, M. F. Insulin receptor substrate proteins and diabetes. *Arch. Pharm. Res.* **27**, 361–370 (2004).
60. Brent, M. M., Anand, R. & Marmorstein, R. Structural Basis for DNA Recognition by FoxO1 and Its Regulation by Posttranslational Modification. *Structure* **16**, 1407–1416 (2008).
61. Brown, M. S., Ye, J., Rawson, R. B. & Goldstein, J. L. Regulated intramembrane proteolysis: A control mechanism conserved from bacteria to humans. *Cell* **100**, 391–398 (2000).
62. Horton, J. D., Goldstein, J. L. & Brown, M. S. SREBPs: activators of the complete program of cholesterol and fatty acid synthesis in the liver. *J. Clin. Invest.* **109**, 1125–31 (2002).
63. Petersen, M. C. & Shulman, G. I. Mechanisms of insulin action and insulin resistance. *Physiological Reviews* **98**, 2133–2223 (2018).
64. Ide, T. *et al.* SREBPs suppress IRS-2-mediated insulin signalling in the liver. *Nat. Cell Biol.* **6**, 351–357 (2004).
65. Honma, M. *et al.* Selective insulin resistance with differential expressions of IRS-1 and IRS-2 in human NAFLD livers. *Int. J. Obes.* **42**, 1544–1555 (2018).
66. Previs, S. F., Withers, D. J., Ren, J. M., White, M. F. & Shulman, G. I. Contrasting effects of IRS-1 versus IRS-2 gene disruption on carbohydrate and lipid metabolism in vivo. *J. Biol. Chem.* **275**, 38990–38994 (2000).



67. Oriente, F. *et al.* Insulin Receptor Substrate-2 Phosphorylation is Necessary for Protein Kinase C $\zeta$  Activation by Insulin in L6hIR Cells. *J. Biol. Chem.* **276**, 37109–37119 (2001).
68. Cohen, P., Alessi, D. R. & Cross, D. A. E. PDK1, one of the missing links in insulin signal transduction? in *FEBS Letters* **410**, 3–10 (John Wiley & Sons, Ltd, 1997).
69. Tessari, P., Coracina, A., Cosma, A. & Tiengo, A. Hepatic lipid metabolism and non-alcoholic fatty liver disease. *Nutrition, Metabolism and Cardiovascular Diseases* **19**, 291–302 (2009).
70. Sanyal, A. J. Mechanisms of disease: Pathogenesis of nonalcoholic fatty liver disease. *Nature Clinical Practice Gastroenterology and Hepatology* **2**, 46–53 (2005).
71. Gerst, F. *et al.* Metabolic crosstalk between fatty pancreas and fatty liver: effects on local inflammation and insulin secretion. *Diabetologia* **60**, 2240–2251 (2017).
72. Samuel, V. T. *et al.* Mechanism of hepatic insulin resistance in non-alcoholic fatty liver disease. *J. Biol. Chem.* **279**, 32345–32353 (2004).
73. Samuel, V. T. *et al.* Inhibition of protein kinase C $\epsilon$  prevents hepatic insulin resistance in nonalcoholic fatty liver disease. *J. Clin. Invest.* **117**, 739–745 (2007).
74. Magkos, F. *et al.* Intrahepatic diacylglycerol content is associated with hepatic insulin resistance in obese subjects. *Gastroenterology* **142**, 1444-1446.e2 (2012).
75. Kumashiro, N. *et al.* Cellular mechanism of insulin resistance in nonalcoholic fatty liver disease. *Proc. Natl. Acad. Sci. U. S. A.* **108**, 16381–16385 (2011).
76. Petersen, M. C. *et al.* Insulin receptor Thr 1160 phosphorylation mediates lipid-induced hepatic insulin resistance Find the latest version : Insulin receptor Thr 1160 phosphorylation mediates lipid-induced hepatic insulin resistance. *J. Clin. Invest.* **126**, 4361–4371 (2016).
77. Kim, J. K. *et al.* Tissue-specific overexpression of lipoprotein lipase causes tissue-specific insulin resistance. *Proc. Natl. Acad. Sci. U. S. A.* **98**, 7522–7527 (2001).
78. Doege, H. *et al.* Silencing of hepatic fatty acid transporter protein 5 in vivo reverses diet-induced non-alcoholic fatty liver disease and improves hyperglycemia. *J. Biol. Chem.* **283**, 22186–22192 (2008).
79. Gabriely, I. *et al.* Removal of visceral fat prevents insulin resistance and glucose intolerance of aging: an adipokine-mediated process? *Diabetes* **51**, 2951–8 (2002).
80. Weiss, R. *et al.* The “Obese Insulin-Sensitive” Adolescent: Importance of Adiponectin and Lipid Partitioning. *J. Clin. Endocrinol. Metab.* **90**, 3731–3737 (2005).
81. Mittendorfer, B., Magkos, F., Fabbrini, E., Mohammed, B. S. & Klein, S. Relationship between body fat mass and free fatty acid kinetics in men and women. *Obesity* **17**, 1872–1877 (2009).
82. Cao, H. *et al.* Regulation of metabolic responses by adipocyte/macrophage fatty acid-binding proteins in leptin-deficient mice. *Diabetes* **55**, 1915–1922 (2006).
83. Jaworski, K. *et al.* AdPLA ablation increases lipolysis and prevents obesity induced by high-fat feeding or leptin deficiency. *Nat. Med.* **15**, 159–168 (2009).
84. Auinger, A. *et al.* A promoter polymorphism in the liver-specific fatty acid transport

- protein 5 is associated with features of the metabolic syndrome and steatosis. *Horm. Metab. Res.* **42**, 854–859 (2010).
85. Lee, H. Y. *et al.* Apolipoprotein CIII overexpressing mice are predisposed to diet-induced hepatic steatosis and hepatic insulin resistance. *Hepatology* **54**, 1650–1660 (2011).
  86. Peter, A. *et al.* Visceral obesity modulates the impact of apolipoprotein C3 gene variants on liver fat content. *Int. J. Obes.* **36**, 774–782 (2012).
  87. Pardina, E. *et al.* Increased Expression and Activity of Hepatic Lipase in the Liver of Morbidly Obese Adult Patients in Relation to Lipid Content. *Obes. Surg.* **19**, 894–904 (2009).
  88. Kim, J. K., Gavrilova, O., Chen, Y., Reitman, M. L. & Shulman, G. I. Mechanism of insulin resistance in A-ZIP/F-1 fatless mice. *J. Biol. Chem.* **275**, 8456–8460 (2000).
  89. Petersen, K. F. *et al.* Leptin reverses insulin resistance and hepatic steatosis in patients with severe lipodystrophy. *J. Clin. Invest.* **109**, 1345–1350 (2002).
  90. Nagle, C. A. *et al.* Hepatic overexpression of glycerol-sn-3-phosphate acyltransferase 1 in rats causes insulin resistance. *J. Biol. Chem.* **282**, 14807–14815 (2007).
  91. Perry, R. J., Samuel, V. T., Petersen, K. F. & Shulman, G. I. The role of hepatic lipids in hepatic insulin resistance and type 2 diabetes. *Nature* **510**, 84–91 (2014).
  92. Neschen, S. *et al.* Prevention of hepatic steatosis and hepatic insulin resistance in mitochondrial acyl-CoA:glycerol-sn-3-phosphate acyltransferase 1 knockout mice. *Cell Metab.* **2**, 55–65 (2005).
  93. Cheol, S. C. *et al.* Suppression of diacylglycerol acyltransferase-2 (DGAT2), but not DGAT1, with antisense oligonucleotides reverses diet-induced hepatic steatosis and insulin resistance. *J. Biol. Chem.* **282**, 22678–22688 (2007).
  94. Lam, T. K. T., Van de Werve, G. & Giacca, A. Free fatty acids increase basal hepatic glucose production and induce hepatic insulin resistance at different sites. *Am. J. Physiol. - Endocrinol. Metab.* **284**, (2003).
  95. Terauchi, Y. *et al.* Glucokinase and IRS-2 are required for compensatory  $\beta$  cell hyperplasia in response to high-fat diet-induced insulin resistance. *J. Clin. Invest.* **117**, 246–257 (2007).
  96. Kubota, N. *et al.* Disruption of insulin receptor substrate 2 causes type 2 diabetes because of liver insulin resistance and lack of compensatory  $\beta$ -cell hyperplasia. *Diabetes* **49**, 1880–1889 (2000).
  97. Sanyal, A. J. *et al.* Nonalcoholic steatohepatitis: Association of insulin resistance and mitochondrial abnormalities. *Gastroenterology* **120**, 1183–1192 (2001).
  98. Vuilleumier, S. Worldwide production of high-fructose syrup and crystalline fructose. *American Journal of Clinical Nutrition* **58**, (1993).
  99. Bray, G. A., Nielsen, S. J. & Popkin, B. M. Consumption of high-fructose corn syrup in beverages may play a role in the epidemic of obesity. *American Journal of Clinical Nutrition* **79**, 537–543 (2004).
  100. Malik, V. S., Schulze, M. B. & Hu, F. B. Intake of sugar-sweetened beverages and weight gain: A systematic review. *American Journal of Clinical Nutrition* **84**, 274–288 (2006).

101. Mattes, R. D. Dietary compensation by humans for supplemental energy provided as ethanol or carbohydrate in fluids. *Physiol. Behav.* **59**, 179–187 (1996).
102. Pan, Y. & Kong, L.-D. High fructose diet-induced metabolic syndrome: Pathophysiological mechanism and treatment by traditional Chinese medicine. *Pharmacol. Res.* **130**, 438–450 (2018).
103. Steenson, S. *et al.* Role of the Enterocyte in Fructose-Induced Hypertriglyceridaemia. *Nutrients* **9**, 349 (2017).
104. Diggle, C. P. *et al.* Kethexokinase: Expression and Localization of the Principal Fructose-metabolizing Enzyme. *J. Histochem. Cytochem.* **57**, 763–774 (2009).
105. Ishimoto, T. *et al.* Opposing effects of fructokinase C and A isoforms on fructose-induced metabolic syndrome in mice. *Proc. Natl. Acad. Sci.* **109**, 4320–4325 (2012).
106. Hayward, B. E. & Bonthron, D. T. Structure and alternative splicing of the kethexokinase gene. *Eur. J. Biochem.* **257**, 85–91 (1998).
107. Katzen, H. M. & Schimke, R. T. Multiple forms of hexokinase in the rat: tissue distribution, age dependency, and properties. *Proc. Natl. Acad. Sci. U. S. A.* **54**, 1218–1225 (1965).
108. Cirillo, P. *et al.* Kethexokinase-Dependent Metabolism of Fructose Induces Proinflammatory Mediators in Proximal Tubular Cells. *J Am Soc Nephrol* **20**, 545–553 (2009).
109. Patel, C. *et al.* Fructose-induced increases in expression of intestinal fructolytic and gluconeogenic genes are regulated by GLUT5 and KHK. *Am. J. Physiol. Regul. Integr. Comp. Physiol.* **309**, R499-509 (2015).
110. Neuschwander-Tetri, B. A. Carbohydrate intake and nonalcoholic fatty liver disease. *Curr. Opin. Clin. Nutr. Metab. Care* **16**, 446–452 (2013).
111. Fernandes-Lima, F., Monte, T. L. R. G., Nascimento, F. A. de M. & Gregório, B. M. Short Exposure to a High-Sucrose Diet and the First ‘Hit’ of Nonalcoholic Fatty Liver Disease in Mice’. *Cells Tissues Organs* **201**, 464–472 (2016).
112. Acosta-Cota, S. de J. *et al.* Histopathological and biochemical changes in the development of nonalcoholic fatty liver disease induced by high-sucrose diet at different times. *Can. J. Physiol. Pharmacol.* **97**, 23–36 (2019).
113. Nomura, K. & Yamanouchi, T. The role of fructose-enriched diets in mechanisms of nonalcoholic fatty liver disease. *J. Nutr. Biochem.* **23**, 203–208 (2012).
114. Stanhope, K. L. *et al.* Twenty-four-hour endocrine and metabolic profiles following consumption of high-fructose corn syrup-, sucrose-, fructose-, and glucose-sweetened beverages with meals. *Am. J. Clin. Nutr.* **87**, 1194–1203 (2008).
115. Bantle, J. P., Ratz, S. K., Thomas, W. & Georgopoulos, A. Effects of dietary fructose on plasma lipids in healthy subjects. *Am. J. Clin. Nutr.* **72**, 1128–1134 (2000).
116. Teff, K. L. *et al.* Dietary fructose reduces circulating insulin and leptin, attenuates postprandial suppression of ghrelin, and increases triglycerides in women. in *Journal of Clinical Endocrinology and Metabolism* **89**, 2963–2972 (J Clin Endocrinol Metab, 2004).
117. Stanhope, K. L. *et al.* Consuming fructose-sweetened, not glucose-sweetened, beverages increases visceral adiposity and lipids and decreases insulin sensitivity

- in overweight/obese humans. *J. Clin. Invest.* **119**, 1322–1334 (2009).
118. Shapiro, A. *et al.* Fructose-induced leptin resistance exacerbates weight gain in response to subsequent high-fat feeding. *Am. J. Physiol. - Regul. Integr. Comp. Physiol.* **295**, R1370 (2008).
  119. Bocarsly, M. E., Powell, E. S., Avena, N. M. & Hoebel, B. G. High-fructose corn syrup causes characteristics of obesity in rats: Increased body weight, body fat and triglyceride levels. *Pharmacol. Biochem. Behav.* **97**, 101–106 (2010).
  120. Youn, J. H., Kaslow, H. R. & Bergman, R. N. Fructose effect to suppress hepatic glycogen degradation. *J. Biol. Chem.* **262**, 11470–11477 (1987).
  121. Thurston, J. H., Jones, E. M. & Hauhart, R. E. Decrease and inhibition of liver glycogen phosphorylase after fructose. An experimental model for the study of hereditary fructose intolerance. *Diabetes* **23**, 597–604 (1974).
  122. Cox, C. L. *et al.* Consumption of fructose- but not glucose-sweetened beverages for 10 weeks increases circulating concentrations of uric acid, retinol binding protein-4, and gamma-glutamyl transferase activity in overweight/obese humans. *Nutr. Metab.* **9**, 68 (2012).
  123. Lanasa, M. A. *et al.* Uric Acid Stimulates Fructokinase and Accelerates Fructose Metabolism in the Development of Fatty Liver. *PLoS One* **7**, e47948 (2012).
  124. Tetri, L. H., Basaranoglu, M., Brunt, E. M., Yerian, L. M. & Neuschwander-Tetri, B. A. Severe NAFLD with hepatic necroinflammatory changes in mice fed trans fats and a high-fructose corn syrup equivalent. *Am. J. Physiol. - Gastrointest. Liver Physiol.* **295**, (2008).
  125. Georgopoulos, A. & Rosengard, A. M. Abnormalities in the metabolism of postprandial and fasting triglyceride-rich lipoprotein subfractions in normal and insulin-dependent diabetic subjects: effects of sex. *Metabolism.* **38**, 781–9 (1989).
  126. Huang, B. W., Chiang, M. T., Yao, H. T. & Chiang, W. The effect of high-fat and high-fructose diets on glucose tolerance and plasma lipid and leptin levels in rats. *Diabetes, Obes. Metab.* **6**, 120–126 (2004).
  127. Crescenzo, R. *et al.* Fructose supplementation worsens the deleterious effects of short-term high-fat feeding on hepatic steatosis and lipid metabolism in adult rats. *Exp. Physiol.* **99**, 1203–1213 (2014).
  128. Messier, C., Whately, K., Liang, J., Du, L. & Puissant, D. The effects of a high-fat, high-fructose, and combination diet on learning, weight, and glucose regulation in C57BL/6 mice. *Behav. Brain Res.* **178**, 139–145 (2007).
  129. Luo, Y. *et al.* Metabolic phenotype and adipose and liver features in a high-fat western diet-induced mouse model of obesity-linked NAFLD. *Am. J. Physiol. - Endocrinol. Metab.* **310**, E418–E439 (2016).
  130. Coate, K. C. *et al.* Chronic consumption of a high-fat/high-fructose diet renders the liver incapable of net hepatic glucose uptake. *Am. J. Physiol. Metab.* **299**, E887–E898 (2010).
  131. Collison, K. S. *et al.* Diabetes of the Liver: The Link Between Nonalcoholic Fatty Liver Disease and HFCS-55. *Obesity* **17**, 2003–2013 (2009).
  132. Ma, X. *et al.* Ghrelin receptor regulates HFCS-induced adipose inflammation and insulin resistance. *Nutr. Diabetes* **3**, e99–e99 (2013).
  133. Meyers, A. M., Mourra, D. & Beeler, J. A. High fructose corn syrup induces

- metabolic dysregulation and altered dopamine signaling in the absence of obesity. *PLoS One* **12**, e0190206 (2017).
134. Browning, J. D. & Horton, J. D. Molecular mediators of hepatic steatosis and liver injury. *J. Clin. Invest.* **114**, 147–152 (2004).
  135. Bollen, M., Keppens, S. & Stalmans, W. Specific features of glycogen metabolism in the liver. *Biochemical Journal* **336**, 19–31 (1998).
  136. Mueckler, M. Facilitative glucose transporters. *Eur. J. Biochem.* **219**, 713–725 (1994).
  137. Van Schaftingen, E., Detheux, M. & Da Cunha, M. V. Short-term control of glucokinase activity: role of a regulatory protein. *FASEB J.* **8**, 414–419 (1994).
  138. van Schaftingen, E. A protein from rat liver confers to glucokinase the property of being antagonistically regulated by fructose 6-phosphate and fructose 1-phosphate. *Eur. J. Biochem.* **179**, 179–184 (1989).
  139. Agius, L. Glucokinase and molecular aspects of liver glycogen metabolism. *Biochemical Journal* **414**, 1–18 (2008).
  140. Turnquist, R. L., Turnquist, M. M., Bachmann, R. C. & Hansen, R. G. Uridine diphosphate glucose pyrophosphorylase: differential heat inactivation and further characterization of human liver enzyme. *BBA - Enzymol.* **364**, 59–67 (1974).
  141. Chiba, H., Ueda, M. & Hirose, M. Purification and properties of beef liver phosphoglucomutase. *Agric. Biol. Chem.* **40**, 2423–2431 (1976).
  142. Roach, P. J. Control of glycogen synthase by hierarchical protein phosphorylation. *FASEB J.* **4**, 2961–2968 (1990).
  143. Ros, S., García-Rocha, M., Domínguez, J., Ferrer, J. C. & Guinovart, J. J. Control of liver glycogen synthase activity and intracellular distribution by phosphorylation. *J. Biol. Chem.* **284**, 6370–6378 (2009).
  144. Ros, S. *et al.* Hepatic overexpression of a constitutively active form of liver glycogen synthase improves glucose homeostasis. *J. Biol. Chem.* **285**, 37170–37177 (2010).
  145. Bultot, L. *et al.* AMP-activated protein kinase phosphorylates and inactivates liver glycogen synthase. *Biochem. J.* **443**, 193–203 (2012).
  146. Wan, M. *et al.* A noncanonical, GSK3-independent pathway controls postprandial hepatic glycogen deposition. *Cell Metab.* **18**, 99–105 (2013).
  147. Cadefau, J., Bollen, M. & Stalmans, W. Glucose-induced glycogenesis in the liver involves the glucose-6-phosphate-dependent dephosphorylation of glycogen synthase. *Biochem. J.* **322**, 745–750 (1997).
  148. Bollen, M., Keppens, S. & Stalmans, W. Differences in liver glycogen-synthase phosphatase activity in rodents with spontaneous insulin-dependent and non-insulin-dependent diabetes. *Diabetologia* **31**, 711–713 (1988).
  149. Newgard, C. B., Hirsch, L. J., Foster, D. W. & McGarry, J. D. Studies on the mechanism by which exogenous glucose is converted into liver glycogen in the rat. A direct or an indirect pathway? *J. Biol. Chem.* **258**, 8046–8052 (1983).
  150. Nilsson, L. H. & Hultman, E. Liver and muscle glycogen in man after glucose and fructose infusion. *Scand. J. Clin. Lab. Invest.* **33**, 5–10 (1974).

151. Katz, J., Kuwajima, M., Foster, D. W. & Denis McGarry, J. The glucose paradox: new perspectives on hepatic carbohydrate metabolism. *Trends in Biochemical Sciences* **11**, 136–140 (1986).
152. Lang, C. H., Bagby, G. J., Blakesley, H. L., Johnson, J. L. & Spitzer, J. J. Plasma glucose concentration determines direct versus indirect liver glycogen synthesis. *Am. J. Physiol. - Endocrinol. Metab.* **251**, (1986).
153. Katz, J. & McGarry, J. D. The glucose paradox. Is glucose a substrate for liver metabolism? *Journal of Clinical Investigation* **74**, 1901–1909 (1984).
154. Newgard, C. B., Moore, S. V., Foster, D. W. & McGarry, J. D. Efficient hepatic glycogen synthesis in refeeding rats requires continued carbon flow through the gluconeogenic pathway. *J. Biol. Chem.* **259**, 6958–6963 (1984).
155. Jarak, I. *et al.* Sources of hepatic glycogen synthesis in mice fed with glucose or fructose as the sole dietary carbohydrate. *Magn. Reson. Med.* **81**, 639–644 (2019).
156. Viegas, I. *et al.* Hepatic glycogen synthesis in farmed European seabass (*Dicentrarchus labrax* L.) is dominated by indirect pathway fluxes. *Comp. Biochem. Physiol. - A Mol. Integr. Physiol.* **163**, 22–29 (2012).
157. Barford, D. & Johnson, L. N. The allosteric transition of glycogen phosphorylase. *Nature* **340**, 609–616 (1989).
158. Carabaza, A., Ciudad, C. J., Baqué, S. & Guinovart, J. J. Glucose has to be phosphorylated to activate glycogen synthase, but not to inactivate glycogen phosphorylase in hepatocytes. *FEBS Lett.* **296**, 211–214 (1992).
159. Alemany, S. & Cohen, P. Phosphorylase a is an allosteric inhibitor of the glycogen and microsomal forms of rat hepatic protein phosphatase-1. *FEBS Lett.* **198**, 194–202 (1986).
160. Massillon, D., Barzilai, N., Chen, W., Hu, M. & Rossetti, L. Glucose regulates in vivo glucose-6-phosphatase gene expression in the liver of diabetic rats. *J. Biol. Chem.* **271**, 9871–9874 (1996).
161. Van Schaftingen, E. & Gerin, I. The glucose-6-phosphatase system. *Biochemical Journal* **362**, 513–532 (2002).
162. Nakayama, A., Yamamoto, K. & Tabata, S. Identification of the Catalytic Residues of Bifunctional Glycogen Debranching Enzyme. *J. Biol. Chem.* **276**, 28824–28828 (2001).
163. Hers, H. G. The control of glycogen metabolism in the liver. *Annu. Rev. Biochem.* **Vol. 45**, 167–189 (1976).
164. Stingl, H. *et al.* Changes in hepatic glycogen cycling during a glucose load in healthy humans. *Diabetologia* **49**, 360–368 (2006).
165. Magnusson, I. *et al.* Liver glycogen turnover in fed and fasted humans. *Am. J. Physiol. - Endocrinol. Metab.* **266**, (1994).
166. Landau, B. R. Methods for measuring glycogen cycling. *American Journal of Physiology - Endocrinology and Metabolism* **281**, 413–419 (2001).
167. Chou, J. Y., Jun, H. S. & Mansfield, B. C. Glycogen storage disease type I and G6Pase- $\beta$  deficiency: Etiology and therapy. *Nature Reviews Endocrinology* **6**, 676–688 (2010).

168. Velho, G. *et al.* Impaired hepatic glycogen synthesis in glucokinase-deficient (MODY-2) subjects. *J. Clin. Invest.* **98**, 1755–1761 (1996).
169. Hwang, J. H. *et al.* Impaired net hepatic glycogen synthesis in insulin-dependent diabetic subjects during mixed meal ingestion: A <sup>13</sup>C nuclear magnetic resonance spectroscopy study. *J. Clin. Invest.* **95**, 783–787 (1995).
170. Byrne, C. D. & Targher, G. NAFLD: A multisystem disease. *Journal of Hepatology* **62**, S47–S64 (2015).
171. Gastaldelli, A. Insulin resistance and reduced metabolic flexibility: Cause or consequence of NAFLD? *Clinical Science* **131**, 2701–2704 (2017).
172. Kneeman, J. M., Misdraji, J. & Corey, K. E. Secondary causes of nonalcoholic fatty liver disease. *Therap. Adv. Gastroenterol.* **5**, 199–207 (2012).
173. Hörsch, D. & Kahn, C. R. Region-specific mRNA expression of phosphatidylinositol 3-kinase regulatory isoforms in the central nervous system of C57BL/6J mice. *J. Comp. Neurol.* **415**, 105–120 (1999).
174. Woods, S. C. & Porte, D. Relationship between plasma and cerebrospinal fluid insulin levels of dogs. *Am. J. Physiol. Endocrinol. Metab. Gastrointest. Physiol.* **2**, (1977).
175. Air, E. L. *et al.* Small molecule insulin mimetics reduce food intake and body weight and prevent development of obesity. *Nat. Med.* **8**, 179–183 (2002).
176. Obici, S., Feng, Z., Karknias, G., Baskin, D. G. & Rossetti, L. Decreasing hypothalamic insulin receptors causes hyperphagia and insulin resistance in rats. *Nat. Neurosci.* **5**, 566–572 (2002).
177. Plum, L., Schubert, M. & Brüning, J. C. The role of insulin receptor signaling in the brain. *Trends in Endocrinology and Metabolism* **16**, 59–65 (2005).
178. Levin, B. E., Dunn-Meynell, A. A. & Routh, V. H. Brain glucose sensing and body energy homeostasis: Role in obesity and diabetes. *American Journal of Physiology - Regulatory Integrative and Comparative Physiology* **276**, (1999).
179. Mayer, J. Glucostatic Mechanism of Regulation of Food Intake. *N. Engl. J. Med.* **249**, 13–16 (1953).
180. Russek, M. Participation of hepatic glucoreceptors in the control of intake of food. *Nature* **197**, 79–80 (1963).
181. Langhans, W., Geary, N. & Scharrer, E. Liver glycogen content decreases during meals in rats. *Am. J. Physiol. - Regul. Integr. Comp. Physiol.* **12**, (1982).
182. Flatt, J. P. Carbohydrate balance and body-weight regulation. *Proc. Nutr. Soc.* **55**, 449–465 (1996).
183. López-Soldado, I. *et al.* Liver glycogen reduces food intake and attenuates obesity in a high-fat diet-fed mouse model. *Diabetes* **64**, 796–807 (2015).
184. López-Soldado, I., Fuentes-Romero, R., Duran, J. & Guinovart, J. J. Effects of hepatic glycogen on food intake and glucose homeostasis are mediated by the vagus nerve in mice. *Diabetologia* **60**, 1076–1083 (2017).
185. Winnick, J. J. *et al.* Hepatic glycogen can regulate hypoglycemic counterregulation via a liver-brain axis. *J. Clin. Invest.* **126**, 2236–2248 (2016).
186. Daniel, I. & Martins Viegas, S. *Sources of blood glucose and liver glycogen in the*

- seabass (Dicentrarchus labrax L.): implications to carbohydrate metabolism in fish.* (2012).
187. Postle, A. D. & Bloxham, D. P. The use of tritiated water to measure absolute rates of hepatic glycogen synthesis. *Biochem. J.* **192**, 65–73 (1980).
  188. Jones, J. G. *et al.* Noninvasive analysis of hepatic glycogen kinetics before and after breakfast with deuterated water and acetaminophen. *Diabetes* **55**, 2294–2300 (2006).
  189. Gil, V. M. S. . G. C. F. G. C. *Ressonância Magnética Nuclear- Fundamentos, Métodos e Aplicações.* (Fundação Calouste Gulbenkian, 2002).
  190. Boggess, B. *Mass Spectrometry Desk Reference (Sparkman, O. David).* *Journal of Chemical Education* **78**, (American Chemical Society (ACS), 2001).
  191. Kanuri, G. & Bergheim, I. In Vitro and in Vivo Models of Non-Alcoholic Fatty Liver Disease (NAFLD). *Int. J. Mol. Sci.* **14**, 11963–11980 (2013).
  192. Takahashi, Y., Soejima, Y. & Fukusato, T. Animal models of nonalcoholic fatty liver disease/ nonalcoholic steatohepatitis. *World Journal of Gastroenterology* **18**, 2300–2308 (2012).
  193. Shimomura, I., Bashmakov, Y. & Horton, J. D. Increased Levels of Nuclear SREBP-1c Associated with Fatty Livers in Two Mouse Models of Diabetes Mellitus. *J. Biol. Chem.* **274**, 30028–30032 (1999).
  194. Nakayama, H. *et al.* Transgenic mice expressing nuclear sterol regulatory element-binding protein 1c in adipose tissue exhibit liver histology similar to nonalcoholic steatohepatitis. *Metabolism.* **56**, 470–475 (2007).
  195. Anstee, Q. M. & Goldin, R. D. Mouse models in non-alcoholic fatty liver disease and steatohepatitis research. *International Journal of Experimental Pathology* **87**, 1–16 (2006).
  196. Farooqi, S., Rau, H., Whitehead, J. & O’Rahilly, S. *ob* gene mutations and human obesity . *Proc. Nutr. Soc.* **57**, 471–475 (1998).
  197. Bray, G. A. & York, D. A. Hypothalamic and genetic obesity in experimental animals: An autonomic and endocrine hypothesis. *Physiological Reviews* **59**, 719–809 (1979).
  198. Chen, H. *et al.* Evidence that the diabetes gene encodes the leptin receptor: Identification of a mutation in the leptin receptor gene in db/db mice. *Cell* **84**, 491–495 (1996).
  199. Wortham, M., He, L., Gyamfi, M., Copple, B. L. & Wan, Y. J. Y. The transition from fatty liver to NASH associates with SAME depletion in db/db mice fed a methionine choline-deficient diet. *Dig. Dis. Sci.* **53**, 2761–2774 (2008).
  200. Schattenberg, J. M. & Galle, P. R. Animal Models of Non-Alcoholic Steatohepatitis: Of Mice and Man. *Dig. Dis.* **28**, 247–254 (2010).
  201. Okumura, K. *et al.* Exacerbation of dietary steatohepatitis and fibrosis in obese, diabetic KK-Ay mice. *Hepatol. Res.* **36**, 217–228 (2006).
  202. PTEN phosphatase and tensin homolog [Homo sapiens (human)] - Gene - NCBI. Available at: <https://www.ncbi.nlm.nih.gov/gene?Db=gene&Cmd=ShowDetailView&TermToSearch=5728#gene-expression>. (Accessed: 21st October 2020)



203. Stiles, B. *et al.* Liver-specific deletion of negative regulator Pten results in fatty liver and insulin hypersensitivity. *Proc. Natl. Acad. Sci. U. S. A.* **101**, 2082–2087 (2004).
204. Horie, Y. *et al.* Hepatocyte-specific Pten deficiency results in steatohepatitis and hepatocellular carcinomas. *J. Clin. Invest.* **113**, 1774–1783 (2004).
205. Vaisse, C. *et al.* Melanocortin-4 receptor mutations are a frequent and heterogeneous cause of morbid obesity. *J. Clin. Invest.* **106**, 253–262 (2000).
206. Huszar, D. *et al.* Targeted disruption of the melanocortin-4 receptor results in obesity in mice. *Cell* **88**, 131–141 (1997).
207. Itagaki, H., Shimizu, K., Morikawa, S., Ogawa, K. & Ezaki, T. Morphological and functional characterization of non-alcoholic fatty liver disease induced by a methionine-choline-deficient diet in C57BL/6 mice. *Int. J. Clin. Exp. Pathol.* **6**, 2683–2696 (2013).
208. Larter, C. Z., Yeh, M. M., Williams, J., Bell-Anderson, K. S. & Farrell, G. C. MCD-induced steatohepatitis is associated with hepatic adiponectin resistance and adipogenic transformation of hepatocytes. *J. Hepatol.* **49**, 407–416 (2008).
209. Ito, M. *et al.* Longitudinal analysis of murine steatohepatitis model induced by chronic exposure to high-fat diet. *Hepatol. Res.* **37**, 50–57 (2007).
210. Deng, Q. G. *et al.* Steatohepatitis induced by intragastric overfeeding in mice. *Hepatology* **42**, 905–914 (2005).
211. Matsuzawa, N. *et al.* Lipid-induced oxidative stress causes steatohepatitis in mice fed an atherogenic diet. *Hepatology* **46**, 1392–1403 (2007).
212. Kawasaki, T. *et al.* Rats fed fructose-enriched diets have characteristics of nonalcoholic hepatic steatosis. *J. Nutr.* **139**, 2067–2071 (2009).
213. Armutcu, F. *et al.* Thymosin alpha 1 attenuates lipid peroxidation and improves fructose-induced steatohepatitis in rats. *Clin. Biochem.* **38**, 540–547 (2005).
214. Spruss, A. *et al.* Toll-like receptor 4 is involved in the development of fructose-induced hepatic steatosis in mice. *Hepatology* **50**, 1094–1104 (2009).
215. Tsuchiya, H. *et al.* High-fat, high-fructose diet induces hepatic iron overload via a hepcidin-independent mechanism prior to the onset of liver steatosis and insulin resistance in mice. *Metabolism.* **62**, 62–69 (2013).
216. Jones, J. *et al.* NMR Derivatives for quantification of 2H and 13C-enrichment of human glucuronide from metabolic tracers. in *Journal of Carbohydrate Chemistry* **25**, 203–217 ( Taylor & Francis Group , 2006).
217. Jones, J. G., Merritt, M. & Malloy, C. Quantifying tracer levels of 2H<sub>2</sub>O enrichment from microliter amounts of plasma and urine by 2H NMR. *Magn. Reson. Med.* **45**, 156–158 (2001).
218. Jones, J. G., Solomon, M. A., Cole, S. M., Sherry, A. D. & Malloy, C. R. An integrated 2H and 13C NMR study of gluconeogenesis and TCA cycle flux in humans. *Am. J. Physiol. - Endocrinol. Metab.* **281**, (2001).
219. Dinunzio, G. *et al.* Determining the contribution of a high-fructose corn syrup formulation to hepatic glycogen synthesis during ad-libitum feeding in mice. *Sci. Rep.* **10**, 12852 (2020).
220. Silva, J. C. P. *et al.* Determining contributions of exogenous glucose and fructose

- to de novo fatty acid and glycerol synthesis in liver and adipose tissue. *Metab. Eng.* **56**, 69–76 (2019).
221. Rito, J. *et al.* Disposition of a Glucose Load into Hepatic Glycogen by Direct and Indirect Pathways in Juvenile Seabass and Seabream. *Sci. Rep.* **8**, 464 (2018).
  222. Keppler and Decker. Determination with amyloglucosidase. *Methods Enzym. Anal.* **3**, 1127–1131 (1974).
  223. Martin, G. J. & Martin, M. L. Deuterium labelling at the natural abundance level as studied by high field quantitative <sup>2</sup>H NMR. *Tetrahedron Lett.* **22**, 3525–3528 (1981).
  224. Delgado, T. C. *et al.* H enrichment distribution of hepatic glycogen from <sup>2</sup>H <sub>2</sub> O reveals the contribution of dietary fructose to glycogen synthesis. *Am J Physiol Endocrinol Metab* **304**, 384–391 (2013).
  225. Shulman, G. I. *et al.* Quantitative comparison of pathways of hepatic glycogen repletion in fed and fasted humans. *Am. J. Physiol. - Endocrinol. Metab.* **259**, (1990).
  226. Galbo, H. & Holst, J. J. The influence of glucagon on hepatic glycogen mobilization in exercising rats. *Pflügers Arch. Eur. J. Physiol.* **363**, 49–53 (1976).
  227. Bizeau, M. E. & Pagliassotti, M. J. Hepatic adaptations to sucrose and fructose. *Metabolism: Clinical and Experimental* **54**, 1189–1201 (2005).
  228. McGuinness, O. P. & Cherrington, A. D. Effects of fructose on hepatic glucose metabolism. *Curr. Opin. Clin. Nutr. Metab. Care* **6**, 441–448 (2003).
  229. Pettit, F. H., Pelley, J. W. & Reed, L. J. Regulation of pyruvate dehydrogenase kinase and phosphatase by acetyl-CoA/CoA and NADH/NAD ratios. *Biochem. Biophys. Res. Commun.* **65**, 575–582 (1975).
  230. Park, S. *et al.* Role of the pyruvate dehydrogenase complex in metabolic remodeling: Differential pyruvate dehydrogenase complex functions in metabolism. *Diabetes and Metabolism Journal* **42**, 270–281 (2018).
  231. Agius, L. & Peak, M. Intracellular binding of glucokinase in hepatocytes and translocation by glucose, fructose and insulin. *Biochem. J.* **296**, 785–796 (1993).
  232. Younossi, Z. *et al.* Nonalcoholic Steatohepatitis Is the Fastest Growing Cause of Hepatocellular Carcinoma in Liver Transplant Candidates. *Clin. Gastroenterol. Hepatol.* **17**, 748-755.e3 (2019).
  233. Portincasa, P., Krawczyk, M., Smyk, W., Lammert, F. & Di Ciaula, A. COVID-19 and non-alcoholic fatty liver disease: Two intersecting pandemics. *Eur. J. Clin. Invest.* **50**, (2020).
  234. Portincasa, P., Krawczyk, M., Machill, A., Lammert, F. & Di Ciaula, A. Hepatic consequences of COVID-19 infection. Lapping or biting? *European Journal of Internal Medicine* **77**, 18–24 (2020).
  235. Lei 30/2019, 2019-04-23 - DRE. Available at: <https://dre.pt/home/-/dre/122151046/details/maximized>. (Accessed: 24th October 2020)